

Automatic differential analysis of NMR experiments in complex samples

Laure Margueritte¹ Petar Markov² Lionel Chiron³
Jean-Philippe Starck³ Catherine Vonthron-Sénécheau¹
Mélanie Bourjot¹ Marc-André Delsuc^{4*}

1. Université de Strasbourg, CNRS, Laboratoire d'Innovation Thérapeutique (LIT), UMR7200, Labex MEDALIS, 67000, Strasbourg, France
2. Structural Biophysics Group, School of Optometry and Vision Sciences, Cardiff University, United Kingdom
3. CASC4DE Le Lodge, 20, Avenue du Neuhof, 67100 Strasbourg, France
4. Institut de Génétique et de Biologie Moléculaire et Cellulaire (IGBMC), INSERM U596, CNRS UMR 7104, Université de Strasbourg, Illkirch-Graffenstaden, France

Abstract

Liquid state NMR is a powerful tool for the analysis of complex mixtures of unknown molecules. This capacity has been used in many analytical approaches: metabolomics, identification of active compounds in natural extracts, characterization of species, and such studies require the acquisition of many diverse NMR measurements on series of samples.

While acquisition can easily be performed automatically, the number of NMR experiments involved in these studies increases very rapidly and this data avalanche requires to resort to automatic processing and analysis.

We present here a program that allows the autonomous, unsupervised processing of a large corpus of 1D, 2D and DOSY experiments from a series of samples acquired in different conditions. The program provides all the signal processing steps, as well as peak-picking and bucketing of 1D and 2D spectra, the program and its components are fully available. In an experiment mimicking the search of an active species in natural extract, we use it for the automatic detection of small amounts of artemisinin added to a series of plant extracts, and for the generation of the spectral fingerprint of this molecules.

This program called Plasmodesma is a novel tool which should be useful to deci-

pher complex mixtures, particularly in the discovery of biologically active natural products from plants extracts, but can also in drug discovery or metabolomics studies.

Introduction

Liquid state NMR is a powerful tool for the analysis of mixtures containing unknown molecules. All species in the solution display their NMR spectra, with a signal intensity proportional to their relative concentrations, provided that slow tumbling rates or relaxation agents do not hide the lines by fast relaxation processes. This capacity has been used in many analytical approaches: metabolomics, identification of active compounds in natural extracts, characterization of species¹⁻⁵. See references (6), (7), and (8) for recent reviews.

Such studies require the acquisition of many diverse NMR measurements on series of samples. Modern NMR spectrometers allow sequential actions (introduction of the sample, probe tuning, acquisition) in order to produce automatically the corresponding 1D and 2D data sets.

Unfortunately, if the acquisition is quite easily performed, the access to the final informations is less straightforward: signal processing (Fourier transform, phasing, baseline correction, peak detection) and finally spectrum interpretation are not trivial tasks. Moreover, the use of 2D spectra implies more complex steps and additional tasks such as reduction of t_1 -noise and t_1 -ridges, or the determination of contour levels for display.

In the case of metabolomics studies, or natural extracts screening, the number of NMR experiments increases very rapidly and this data avalanche requires to resort to automatic processing. While metabolomics are aimed at measuring precisely the amount of well-known compounds, and to quantify precisely their variations from sample to sample, the identification of an active molecule in a natural extracts starts with its detection and then its characterization of an unknown compound or eventually a family of related species.

In this article, we present the specific development of a computer program allowing the autonomous, unsupervised processing of a large corpus of 1D and 2D experiments from a series of samples acquired in different conditions.

Results obtained using this program on series of complex natural extracts highlight the time saving and the efficiency increase regarding classical “hand-made” processing of raw data.

Software developments

Plasmodesma

The program Plasmodesma⁹ developed for this project relies on the SPIKE library for most of its operation¹⁰. It is intended to process autonomously a large series of different spectra originated from different samples, obtained in varying conditions. This analytical process involves the handling of a complex set of NMR experiments (1D and 2D homo- or hetero-nuclear spectra), at the end, a spectral report summarizing the analysis is expected, containing all figures, peak and bucket lists for each sample.

The current work is based on SPIKE (**S**pectrometry **P**rocessing **I**nnovative **K**ernel) a comprehensive software on which the current work is based, is a comprehensive software library aimed at the processing and analysis of Fourier transform spectroscopies. It provides basic functionalities such as apodization, Fourier transforms, phasing, peak-picking, line-fitting, baseline correction as well as more advanced tools. It is easily extensible through a plug-in mechanism. SPIKE combines the use of a parallel multi processor approach to a low memory footprint, thus insuring rapid processing with an optimal use of the computer hardware. Moreover, SPIKE allows the efficient handling and visualization of very large data-sets limited only by disk space. SPIKE is a continuation of the previous Gifa and NPK^{11,12} NMR processing softwares, and was developed to include other Fourier transform spectroscopies, in particular FT Mass spectrometry (Orbitrap and FT-ICR) and 2D-FT-ICR¹³⁻¹⁵. For portability reasons and ease of development, the program is written in Python, and relies on external libraries such as `numpy`, `scipy`, `pandas`, and `hdf5`.¹⁶⁻²⁰

Principle of operations

The program Plasmodesma operates without any human interaction. When applied to a folder, all NMR files are imported, processed, and a global report is generated for the totality of the analysis. All the processing and analysis steps are optimized depending on the acquisition parameters found in the data-sets, either 1D or 2D data. No other input is required. The 1D and 2D experiments are processed sequentially, The data are apodized, Fourier transformed, and the baseline corrected, 1D spectra are also automatically phased. Additionally, an efficient denoising step²¹ is performed on the 2D experiments, in order to reduce the t_1 -noise. The F1 Fourier transform step of the 2D data-sets is performed depending on the spectral type and on the acquisition protocol. The calibration is then determined precisely from the reference signal (in this case, 0 ppm for the TMS). A peak-picking and bucket analysis are then performed (see below). Peak lists and bucket lists are generated as csv files for each experiment. Finally, figures of each spectrum is created, with and without peaks displayed. A final

report that contains all acquisition and processing parameters is generated (see S.I. S1).

Specific developments

Some functions used by Plasmodesma have been developed specifically for this analysis, and were implemented as SPIKE plug-ins.

Autophasing

In the context of metabonomics and screening studies, the possibility to detect and quantify precisely the intensity of vanishing small peaks is paramount. The phase of a 1D spectrum, if set slightly off, may have a strong impact on the possibility to detect small signals, in particular if they are close to a large one. Errors of only a few degrees introduce bias resulting to too low or too high quantization, as well as shifts of the maximum. Automatically acquired natural extract spectra are usually difficult to phase because of strong solvent lines and other artifacts present in the spectra. The improvement of the simple but robust automatic phasing procedure developed in NPK¹² contributes efficiently to resolve this problem. The principle is to minimize the negative wing of the 1D spectrum, by performing a grid search first on 0th order (frequency independent) alone, then on both 0th and 1st order (frequency dependent) corrections, the larger peak being used as the 1st order pivot. An automatic baseline correction (see below) is performed at each correction step, and an optional *inwater* mode allows to ignore the central spectral zone.

Autobaseline

A flat baseline is also a requisite for correct analysis, and a specific plugin as been developed in this respect. We developed a new approach, which relies on an iterative statistical treatment on the signal split into pieces of constant length, and fitting the baseline by piecewise linear segments. The fit is based on the use of a linear regression minimizing the $\ell_p(x) = (\sum(|x|^p))^{1/p}$ norm of the difference. A rough estimate of the spectral baseline is first generated using $p = 1$ on each pieces. Then, the estimate is iteratively improved by removing that part of the signal above the current baseline approximation, and using $p = 3$ for fitting. This method guarantees baselines that stick well to the signal avoiding spurious oscillations that higher-order polynomials or splines may produce.

Bucketing

Bucketing is an important operation in the processing pipeline. It consists in computing the area under the spectrum over small spectral segments which cover

the whole spectral width. The segments should be large enough to blur the small discrepancies that appear from one sample to another, while preserving the resolutive power of the spectra. A bucket size of 0.01 ppm was used for 1D ^1H spectra.

Bucketing also reduces the size of the data that will be submitted to statistical analysis. This is of foremost importance in the analysis of 2D spectra, which routinely contains millions of points. The reduction of 2D datasets to tractable sizes in statistical tools requires nevertheless bucket sizes on the order of 0.03 to 0.05 ppm in ^1H spectroscopy and to 1.0 ppm in ^{13}C . Such sizes are certainly too large to capture all the details contained in the 2D spectra. One solution to this difficulty could be to use segments of varying size, however we rather chose to enrich the information by adding to the area of each bucket, additional information. For each bucket, computed over 1D or 2D spectra, the coordinates of the bucket center and its size in pixel were stored, along with the area information computed as the mean over the bucket, and enriched with the values of the min and max points, and the standard deviation of data over the bucket.

Processing of DOSY experiment

DOSY spectra are extremely efficient in deciphering complex mixtures, and have been used in many different work (see *Mahrous et al*⁷ and reference therein). They require a specific processing for the analysis of the exponential decays observed along the indirect dimension of the 2D spectrum. In this work this specific processing was performed by using the recently introduced PALMA algorithm²² that implements a rapid Inverse Laplace Transform analysis, using a hybrid constraint, maximizing the entropy while minimizing the ℓ_1 norm of the reconstructed spectrum. This algorithm was developed using the SPIKE library, so it was particularly easy to insert it into the processing pipe-line. As a consequence, they are systematically processed and a peak list and an adapted bucket list is also generated.

Report

Finally, a concise report is produced as a csv file (see S.I. S2). The report contain all the important parameters related to data acquisition and processing. They are finally displayed, as rendered using the pandas python library¹⁸.

Analysis

Given a set of 1D and 2D NMR raw experiments, the approach described above is able to produce, in full automation and without any human interaction, a set of correctly processed spectra, along with complete peak lists and enriched bucket lists.

The artifacts observed in the spectra, such as antidiagonals, t_1 noise and ridges, etc. were corrected on the bucket list. On modern spectrometers these artifacts are usually at a low intensity, however as the purpose here is to detect species at low concentration, and their presence is detrimental.

The 2D bucket list is corrected for remaining t_1 noise and t_1 ridges for each column in the matrix, by setting to null all buckets below twice the median value of the considered column. The bucket list originated from symmetric spectra, such COSY and TOCSY, were further corrected for departure of this symmetry by setting symmetrical buckets to the minimum value of the pair. These two operations have the effect of preserving the most significant buckets, without losing the weak spectral areas.

M&M

Chemicals. Artemisinin 98% was purchased in Sigma-Aldrich and deuterated methanol (10 x 0.75mL) in Eurisotop (Saint Aubin, France).

Algae collection and identification. The algae *Sargassum muticum* was collected in June 2006 in Cap Lévy (Manche), France. Taxonomic determination was performed by Dr A-M. Rusig and a voucher specimen was deposited in the Herbarium of the University of Caen. Extraction was realized as in Vonthron-Sénécheau et al.²³.

Samples preparation. Five samples containing 10 mg of *S. muticum* hydroalcoholic extract were prepared. An artemisinin DMSO solution at 3 mg/mL was added to the samples to obtain a final concentration of artemisinin of 0.2, 0.3, 0.4 and 2.7 mg/ml in NMR tubes, as summarized in Table 1. All samples were lyophilized and dissolved in 750 μ L of methanol d4, and put in 5 mm NMR tubes. The NMR tubes were spun with a small bench centrifuge to help sedimentation of insoluble parts, and placed in the NMR sample changer.

Table 1: Samples preparation

Sample n°	1	2	3	4	5
<i>S. muticum</i> extract	10 mg	10 mg	10 mg	10 mg	10 mg
added artemisinin	0 mg	0.15 mg	0.24 mg	0.32 mg	2 mg

A sample of pure artemisinin was prepared in methanol d4 and studied by NMR.

NMR spectroscopy

Acquisitions were performed on a Bruker Avance-III spectrometer operating at 700 MHz, and equipped with a TCI cryo probe and a standard Bac60 sample

changer. Each sample was automatically inserted into the spectrometer, tuned and shimmed after a stabilization delay of 120 seconds. All experiments were automatically run on each sample, the whole sequence being programmed using a TopSpin macro (see E.S.I S2). Spectral parameters ($\pi/2$ pulses, receiver gain. . .) were optimized on one sample and used for the whole series without further check.

Spectral widths were set to 12 ppm in ^1H and to 150 ppm in ^{13}C . 1D spectra were acquired on 64 scans, 16384 points, and a relaxation delay of 1.5 sec, for a total time of 3 minutes. COSY experiments were performed with 8 scans, with 512 increments of 4096 points each, for a total acquisition time of 2 hours. TOCSY experiments were performed with 8 scans, with 400 increments of 4096 points each, and using a DISPSI-2 mixing sequence of 80 msec duration. TOCSY acquisition time was 1 hour 40 minutes. DOSY experiments were performed with 32 scans, with 50 increments of 4096 points each, for a total acquisition time of 50 minutes. HSQC experiments were performed with 4 scans, with 512 increments of 2048 points each, for a total acquisition time of 1 hour. HMBC experiments were performed with 48 scans, with 400 increments of 4096 points each, for a total acquisition time of 10 hours.

The complete acquisition time for one sample, including sample injection and tuning, took about 16 hours. The five samples were acquired in one continuous run.

The artemisinin sample was studied by NMR: Artemisinin: ^1H NMR (CD₃OD, 700 MHz) δ 0.99 (3H, d, $J = 6.2$ Hz, 6-CH₃), 1.16 (3H, d, $J = 7.2$ Hz, 9-CH₃), 1.38 (3H, s, 3-CH₃), 2.08 (1H, ddd, H4), 2.40 (1H, ddd, H4), 2.01 (1H, m, H5), 1.47 (1H, m, H5), 1.38 (1H, m, H5a), 1.52 (1H, m, H6), 1.09 (1H, m, H7), 1.77 (1H, m, H7), 1.17 (1H, m, H8), 1.86 (1H, m, H8), 1.82 (1H, m, H8a), 3.31 (1H, dq, H9), 6.03 (1H, dq, H12), ^{13}C NMR (CD₃OD, 700 MHz) δ 106.7 (C, C3), 25.2 (CH₃, C3), 36.6 (CH₂, C4), 25.7 (CH₂, C5), 51.2 (CH, C5a), 38.1 (CH, C6), 19.9 (CH₃, C6), 34.6 (CH₂, C7), 24.0 (CH₂, C8), 45.6 (CH, C8a), 34.0 (CH, C9), 12.7 (CH₃, C9), 81.0 (CH, C12a), 95.5 (CH, C12).

Data Processing

Spectral Processing was integrally performed using the Plasmodesma program presented here. The program is written in python, and is compatible both with python 2 and python 3. It is based on the SPIKE library¹⁰ and the DOSY processing were performed using the PALMA approach²² embedded in SPIKE as a plugin.

Complete processing took 96 minutes on a MacOs machine, running the python anaconda distribution 4.2 from Continuum Analytics (Austin, TX).

Statistical Analysis. The bucket lists and peak lists produced by the Plasmodesma run were analyzed with a python script based on the pandas library,

using the Jupyter notebook environment.

The Plasmodesma program, along with examples, experimental data related to the artemisin series, Jupyter notebooks presenting the data analysis, and the specific SPIKE plugins are freely available at <https://github.com/delsuc/plasmodesma> repository.

Results

To mimic the presence of a bioactive molecule at different concentrations in complex mixtures, crude plant extracts were supplemented at different concentrations with artemisinin, a naturally occurring and structurally known sesquiterpene lactone, and five different samples were prepared. All five samples were placed in the sample changer and NMR data were acquired in an automatic manner, after an initial tuning of the first sample.

Data Processing

The raw data-sets were processed as described above, and the peak lists and bucket lists generated. Figures 1 and 2 show an example of the result of such a processing.

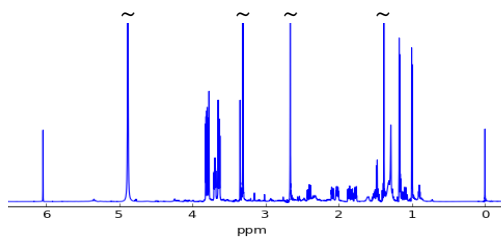


Figure 1: 1D ^1H spectrum of sample n°5.

The bucketing procedure is used to summarize the spectral content, and by reducing the size of the data to handle, to ease further statistical analysis. However, it can be seen in Figure 2 that t_1 -noise and other spectral artifacts are present in particular in the standard deviation analysis, which enhances the local signal variations. It appears that corruption of buckets from spectral artifacts appear more deleterious in 2D spectroscopy than in classical 1D. For this reason, the areas and standard deviation values of the bucket list were subjected to the simple procedures described above. The first step consists in setting to a null value all values below a certain threshold computed from the median over the vertical column of the considered bucket. This procedure allows to remove a large part of the noise, and to only retain the peaks separated above the threshold.

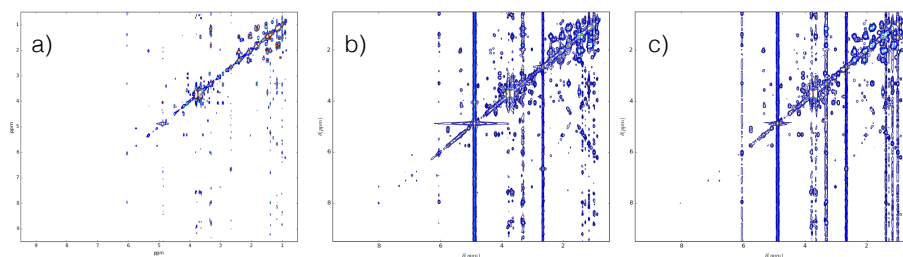


Figure 2: COSY spectrum of sample n°5. a) automatically generated contour plot, b) graphic representation of the raw bucket list, c) same as b, but showing the standard deviation of each bucket.

The threshold level adapted for each column permit to efficiently clean the strong t_1 -noise stripes, while preserving weak peaks located in less crowded regions. In a second step, homonuclear experiments a symmetrization procedure can be applied, it was done here by simply taking the smaller of the two values related by symmetry. This procedure is much simpler and more robust on bucket lists than on real spectra, as the bucketing has already homogenized the spectral axes and produced squared buckets. This procedure was applied on the area and the standard deviation values of the bucket list.

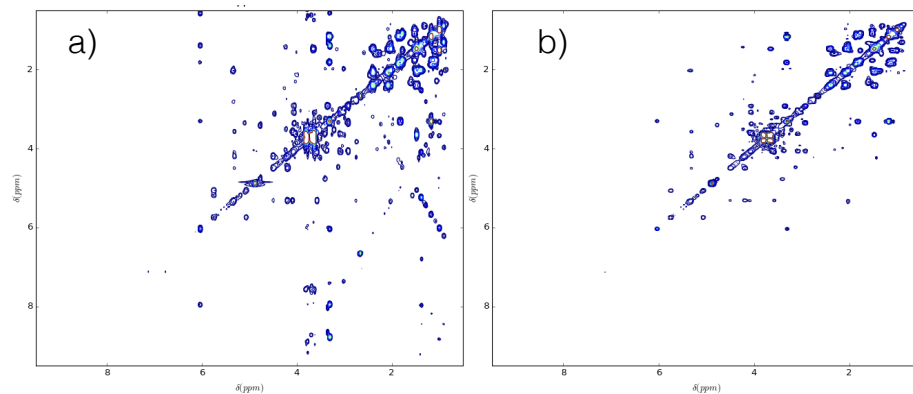


Figure 3: a) Standard deviation the bucket list from Figure 2 after t_1 -noise removal, b) same data as in a) after symmetrization.

Figure 3 shows the result of each cleaning steps. It can clearly be seen that this procedure, allows an improvement of the quality of data and a better compatibility with automatic analysis.

Data Analysis

The cleaned bucket lists can be efficiently used for detection of the spectral features varying from spectrum to another. This can be done on any 1D or 2D spectra: Figure 4 shows the result on the analysis of the COSY spectrum.

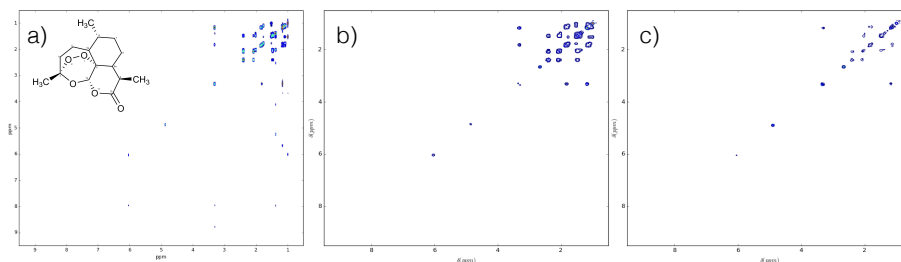


Figure 4: Automatic extraction of spectral fingerprint from the automatic spectral analysis a) standard COSY spectrum of artemisinin, b) result of the subtraction of the std channel of the bucket lists of sample 5 and sample 1, c) same as b) for sample 4 and sample 1.

Obviously, the positions of the signals of the artemisinin spectrum is detected and separated from the constant background, even though the background is of much larger intensity. Here the original spectrum is not genuinely recovered, not only because some signals are missing, but principally because of the loss of the intensities. However, the generated spectral pattern can be used to extract chemical shifts and topologies, and recognize a molecular pattern, which can be used as a fingerprint. The same result cannot be obtained directly from the spectrum, and is efficient because the bucketing standardizes the spectra, the standard deviation measures the fluctuation rather the intensity. Finally the cleaning operation smooth out the random fluctuations which otherwise would hamper the direct comparison to operate.

The procedure above is not very sensitive, and the samples with lower level of added artemisinin could not be processed efficiently. A second procedure was tested by taking the ratio of the bucket standard deviation values. The results are shown in Figure 5: despite a low level of concentration (few hundred micrograms of artemisinin in 10 mg of crude material), the spectral fingerprint is recovered. In this case the diagonal of the homonuclear spectrum is not recovered, this does not have a strong impact, as it can be fully inferred from the off-diagonal fingerprint dots.

Linear regression

This first approach take spectra two by two, and can be used on homonuclear spectra, as shown here, and also on heteronuclear ones. Using the whole set of

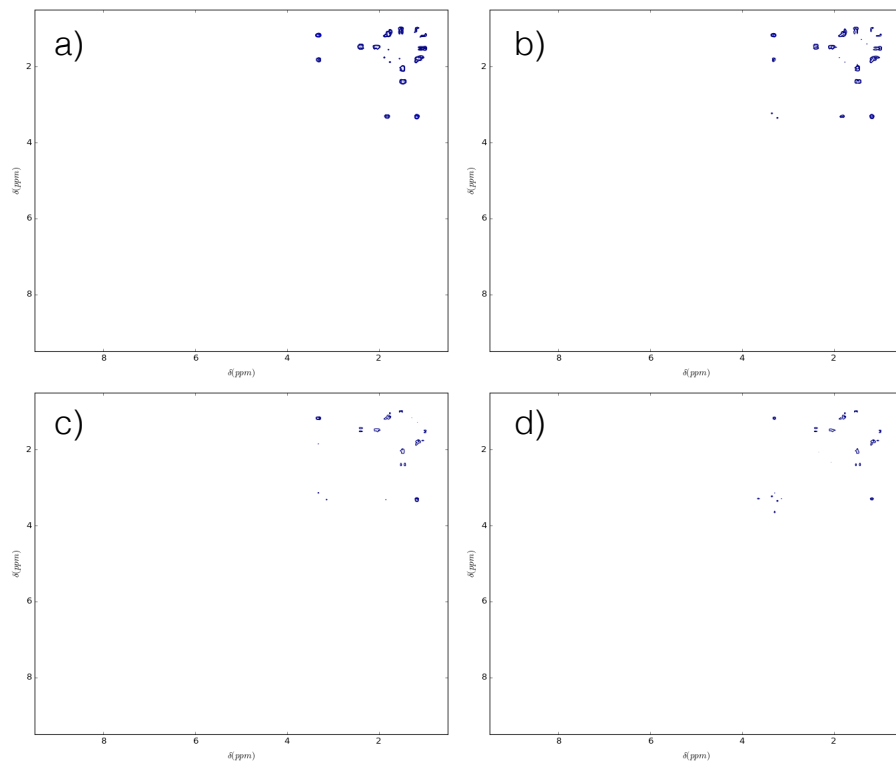


Figure 5: Spectral fingerprint obtained by the ratio of bucket standard deviation, a) comparison of sample 5 and sample 1, b-c-d) same as a for sample 4, 3 and 2 respectively.

spectra at once requires to have an additional information, eventually imprecise, on the amount of active material in each sample. In this case, signals coming from the studied molecule are expected to be proportional to its concentration, and this property can be exploited to separate those signals, varying along with the concentration value, to the other signal, uncorrelated with it. This was performed by using the `scikit-learn` library²⁴, a generic tool for machine learning, written in python with full interoperability with python, Jupyter and SPIKE. The `linear_model.LinearRegression()` function and the Recursive Feature Elimination tool were used, and applied on the the bucket lists area values (see S.I. for detailed operation).

These tools allow to select a small subset of parameters which best correlate with the estimated concentration. The selected features are then supposed to define a spectral fingerprint in a manner equivalent with the previous approach, but with a quantitative aspect this time. As the whole spectrum series is used, it is expected to produce better results. Results are shown in Figure 6 for the HSQC spectra obtained on the 4 samples presenting the lowest concentration. It can be seen that the HSQC spectrum of artemisinin is extracted from the complex spectrum of the mixture. The main artifacts observed in the fingerprint are associated with the solvent lines (here water, methanol and DMSO)

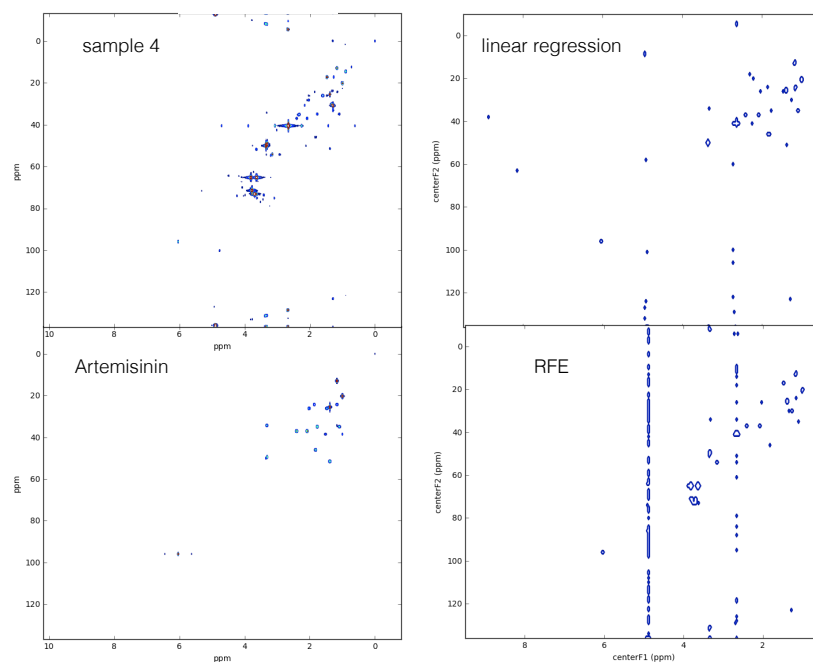


Figure 6: HSQC Spectral fingerprint determined from the linear regression analysis over the 4 samples with lowest concentration.

Discussion

The measurement of NMR spectra over series of complex samples, and their analysis, is a common procedure in screening or activity studies. The acquisition part is usually well covered through the use of sample changers and associated softwares, with the eventual help of companion programs, allowing an optimized set-up²⁵. Here, we extend the set of tools for these studies to the possibility of automatic processing and statistical analysis of the set of 1D and 2D spectra. There are already basic tools which allow to perform the first processing steps of the data, however, they usually rely either on preset parameters values (phase corrections, window function) or crude estimate of the optimum parameters (baseline correction). In contrast, the program *Plasmodesma* presented here, works in an autonomous manner, without any user interaction, relying on a small set of preset global parameters. It is able to autonomously process 1D, 2D, and DOSY experiments, processing parameters are optimized either from the experiment types (window function) or optimized automatically on the data (phase correction, baseline). In addition, advanced methods are used for the denoising of 2D spectra or the analysis of DOSY experiments. Finally, the program generates spectra and peak lists and bucket lists for all spectra, as well as reports on the data and the analysis.

The use of the *SPIKE* library¹⁰, a generalist processing library for NMR and other Fourier spectroscopies, allowed a rapid development of the program, as well as the use of advance tools. Not relying on parameters previously by an operator allow to process directly after the measure, and use the result of the processing as a token for the quality of the acquisition. The processing step being more rapid than the acquisition, it is perfectly possible to repeat the processing along the series of measurements, to monitor the advance and quality of the current experiment.

The series of spectra are further algorithmically analyzed using machine-learning inspired approaches. However, each 2D spectrum is typically composed of several million of data points, and this size hampers the possibility to algorithmically compare efficiently several spectra. For instance the series of spectra generated in this study represents more than 20 million points overall, and some pre-conditioning of the data is required. For this reason, the automatic analysis of the spectra is here principally performed on the bucket lists, which provided a reduced but faithful representation of the spectrum. Many artifacts such as antidiagonals, t_1 noise and ridges, are also present. These artifacts are of rather low intensity, however as the purpose here is the detection of compounds at low concentration, their presence is detrimental, and we chose to correct them on the bucket list rather than on the original spectra. This smoothing and spectral normalization afforded by the bucketing operation allows optimal spectral corrections and makes comparison between spectra obtained from different samples easier. Finally, access to quantities such as standard deviation of the signal, min and max values, allows a finer description of the spectra.

From this material, a spectral fingerprint of the searched molecule could be first determined from a two-by-two comparison of spectra with a presence/absence of the searched compound, In this case the approach consisting in comparing by ratio the standard deviation of buckets from spectra of COSY type showed to be able to detect and extract the spectral features of the compound even at low concentrations. Linear regression over the whole series of spectra was also used to generate a faithful fingerprint. One step regression as well as recursive feature selection were used, and both proved to be efficient in extracting a spectral fingerprint for both homonuclear and heteronuclear experiments (see figure 6 and S.I. S2).

Each experiment types can be used for the determination of the fingerprint, and COSY type and HSQC type experiments were explored. It is possible to perform the same analysis on a concatenation of all experiments, however such an approach did not provide a correct result, probably because of the heterogeneity of the different spectra types.

Conclusion

The program developed in this work represents an efficient alternative for the autonomous processing of a series of NMR data (1D and 2D) and contributes efficiently to the discovery of structurally unknown molecules present in natural extracts, without any chromatographic separation. It fully exploits the NMR technique as a fingerprinting technique: complete 2D NMR fingerprint of the compound is recovered through differential analysis performed both by comparison of local variation in the spectra or by linear regression between signal intensity and the concentrations of the natural product in the sample.

The extended bucketing procedure allows a strong reduction of the size of the data, while preserving a large part of the molecular information present in the original spectra. Basic machine learning approaches were used to analyze this compressed but rich information, and proved sufficient to readily extract the spectral fingerprint of the unknown molecule, either from spectral comparison, or by handling of the whole spectral series at once.

Plasmodesma is a novel tool which should be useful to decipher complex mixtures, particularly in the discovery of biologically active natural products from plants extracts, but can also in drug discovery or metabolomics studies.

Acknowledgments

The authors are very grateful to Labex Medalis and Région Alsace for a fellowship (LM), and Europe for an Erasmus fellowship (PM). We are also grateful to A-M.Rusig for the collect and the identification of the algal material, J.Viéville

for help in the NMR set-up, and G.Bret for help in the statistical analysis. We acknowledge Wikimedia²⁶ for the *S.muticum* picture used in the Graphical Abstract.

E.S.I.

- S1 Processing of the artemisinin series
- S2 Analysis of the artemisinin series

References

- [1] Bakiri, A.; Hubert, J.; Reynaud, R.; Lanthony, S.; Harakat, D.; Renault, J.-H.; Nuzillard, J.-M. *J Nat Prod.* **2017**, *80* (5), 1387–1396.
- [2] D’Abrosca, B.; Lavorgna, M.; Scognamiglio, M.; Russo, C.; Graziani, V.; Piscitelli, C.; Fiorentino, A.; Isidori, M. *Food Chem Toxicol.* **2017**.
- [3] Abdelsalam, A.; Mahran, E.; Chowdhury, K.; Boroujerdi, A.; El-Bakry, A. *Physiol Mol Biol Plants.* **2017**, *23* (2), 369–383.
- [4] Hubert, J.; Nuzillard, J.-M.; Purson, S.; Hamzaoui, M.; Borie, N.; Reynaud, R.; Renault, J.-H. *Anal Chem.* **2014**, *86* (6), 2955–2962.
- [5] Oetl, S.-K.; Hubert, J.; Nuzillard, J.-M.; Stuppner, H.; Renault, J.-H.; Rollinger, J.-M. *Anal Chim Acta.* **2014**, *846*, 60–67.
- [6] Larive, C. K.; Barding Jr, G. A.; Dinges, M. M. *Anal Chem* **2015**, *87* (1), 133–146.
- [7] Mahrous, E.; Farag, M. *J Adv Research* **2015**, *6* (315).
- [8] Wolfender, J.-L.; Marti, G.; Thomas, A.; Bertrand, S. *J Chromatogr A.* **2015**, *1382*, 136–164.
- [9] Wikipedia. “*Plasmodesma are microscopic channels which traverse the cell walls of plant cells and some algal cells, enabling transport and communication between them*”. <https://en.wikipedia.org/wiki/Plasmodesma>, [Online; accessed 16-May-2017].
- [10] Chiron, L.; Coutouly, M.-A.; Starck, J.-P.; Rolando, C.; Delsuc, M.-A. *arXiv* **2016**.
- [11] Pons, J. L.; Malliavin, T. E.; Delsuc, M.-A. *J Biomol NMR* **1996**, *8*, 445–452.
- [12] Tramesel, D.; Catherinot, V.; Delsuc, M.-A. *J Magn Reson* **2007**, *188* (1), 56–67.
- [13] Pfändler, P.; Bodenhausen, G.; Rapin, J.; Houriet, R.; Gäumann, T. *Chem*

Phys Let **1987**, *138* (2), 195–200.

[14] Pfändler, P.; Bodenhausen, G.; Rapin, J.; Walser, M.; Gäumann, T. *J Am Chem Soc* **1988**, *110* (17), 5625–5628.

[15] van Agthoven, M. A.; Delsuc, M.-A.; Bodenhausen, G.; Rolando, C. *Anal Bioanal Chem* **2013**, *405*, 51–61.

[16] van der Walt, S.; Colbert, S.; Varoquaux, G. *Comput Sci Eng* **2011**, *13*, 22–30.

[17] Jones, E.; Oliphant, T.; Peterson, P.; Others. SciPy: Open source scientific tools for Python, 2001.

[18] McKinney, W. *Pandas, Python Data Analysis Library. 2015*; Reference Source, 2014.

[19] The HDF Group. Hierarchical Data Format, version 5.

[20] Alted, F.; Vilata, I.; others. PyTables: Hierarchical datasets in Python, 2002.

[21] Chiron, L.; van Agthoven, M. A.; Kieffer, B.; Rolando, C.; Delsuc, M.-A. *Proc Natl Acad Sci USA* **2014**, *111* (4), 1385–1390.

[22] Cherni, A.; Chouzenoux, E.; Delsuc, M.-A. *Analyst* **2017**, *142* (5), 772–779.

[23] Vonthron-Sénécheau, C.; Kaiser, M.; Devambe, I.; Vastel, A.; Mussio, I.; Rusig, A.-M. *Mar. Drugs* **2011**, *9*, 922–933.

[24] Pedregosa, F.; Varoquaux, G.; Gramfort, A.; Michel, V.; Thirion, B.; Grisel, O.; Blondel, M.; Prettenhofer, P.; Weiss, R.; Dubourg, V.; Vanderplas, J.; Passos, A.; Cournapeau, D.; Brucher, M.; Perrot, M.; Duchesnay, E. *Journal of Machine Learning Research* **2011**, *12*, 2825–2830.

[25] Clos, L. J.; Jofre, M. F.; Ellinger, J. J.; Westler, W. M.; Markley, J. L. *Metabolomics* **2013**, *9* (3), 558–563.

[26] Commons, W. File:Sargassum muticum yendo fensholt 1955 lamiot wimereuxhautsdefrance estran juillet 2016a9.jpg — wikimedia commons, the free media repository, 2016.

Supp.Info 1

Supporting Information

Automatic differential analysis of NMR experiments in complex samples

Laure Margueritte, Petar Markov, Lionel Chiron, Jean-Philippe Starck, Catherine Vonthron-Sénécheau, Mélanie Bourjot, Marc-André Delsuc*

Spectra of sample 1 :

S1 - ^1H NMR spectrum (MeOD, 700 MHz)

S2 - COSY spectrum (MeOD, 700 MHz)

S3 - TOCSY spectrum (MeOD, 700 MHz)

S4 - HSQC spectrum (MeOD, 700 MHz)

S5 - HMBC spectrum (MeOD, 700 MHz)

S6 - DOSY spectrum (MeOD, 700 MHz)

Spectra of sample 2 :

S7 - ^1H NMR spectrum (MeOD, 700 MHz)

S8 - COSY spectrum (MeOD, 700 MHz)

S9 - TOCSY spectrum (MeOD, 700 MHz)

S10 - HSQC spectrum (MeOD, 700 MHz)

S11 - HMBC spectrum (MeOD, 700 MHz)

S12 - DOSY spectrum (MeOD, 700 MHz)

Spectra of sample 3 :

S13 - ^1H NMR spectrum (MeOD, 700 MHz)

S14 - COSY spectrum (MeOD, 700 MHz)

S15 - TOCSY spectrum (MeOD, 700 MHz)

S16 - HSQC spectrum (MeOD, 700 MHz)

S17 - HMBC spectrum (MeOD, 700 MHz)

S18 - DOSY spectrum (MeOD, 700 MHz)

Spectra of sample 4 :

S19 - ^1H NMR spectrum (MeOD, 700 MHz)

S20 - COSY spectrum (MeOD, 700 MHz)

S21 - TOCSY spectrum (MeOD, 700 MHz)

S22 - HSQC spectrum (MeOD, 700 MHz)

S23 - HMBC spectrum (MeOD, 700 MHz)

S24 - DOSY spectrum (MeOD, 700 MHz)

Spectra of sample 5 :

S25 - ^1H NMR spectrum (MeOD, 700 MHz)

S26 - COSY spectrum (MeOD, 700 MHz)

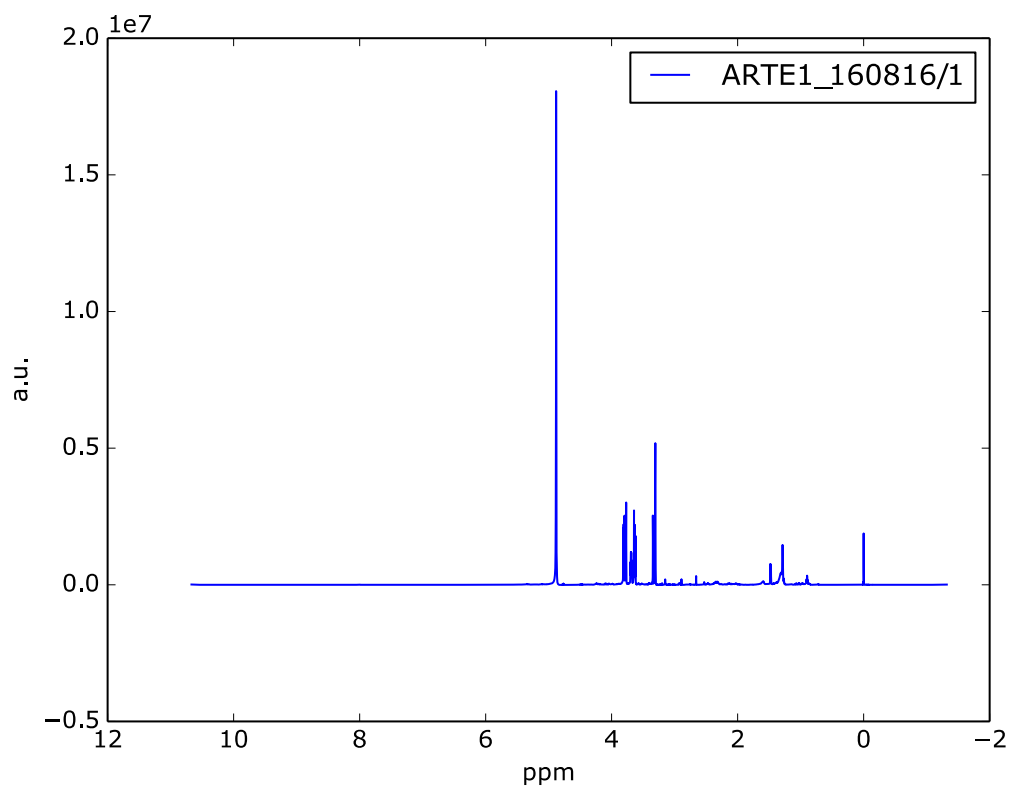
S27 - TOCSY spectrum (MeOD, 700 MHz)

S28 - HSQC spectrum (MeOD, 700 MHz)

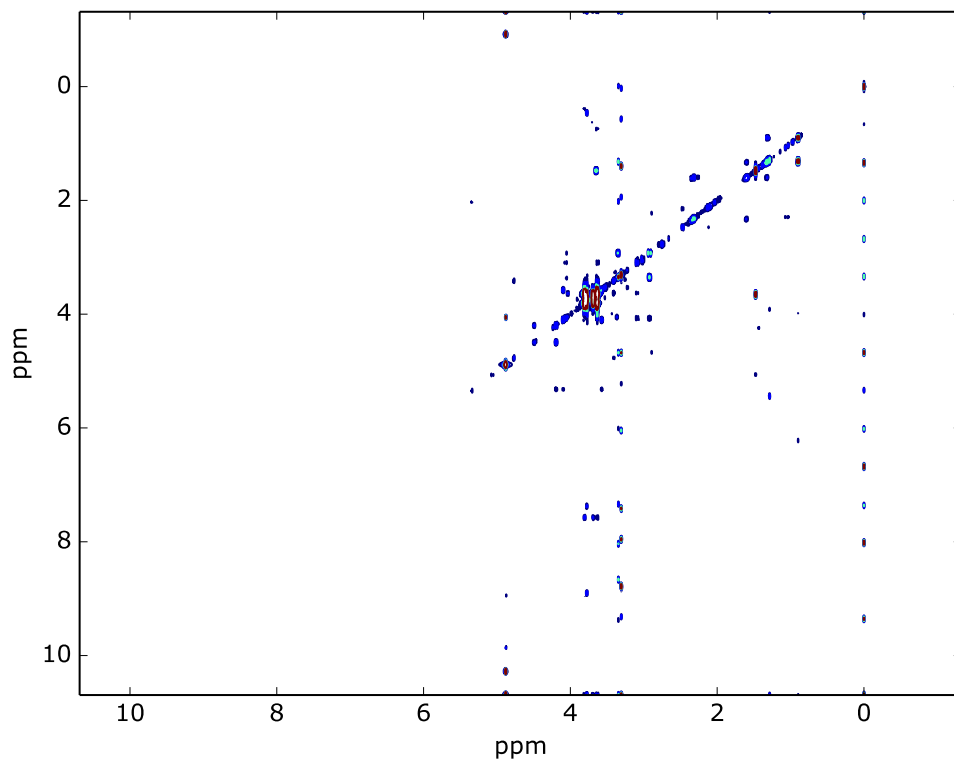
S29 - HMBC spectrum (MeOD, 700 MHz)

S30 - DOSY spectrum (MeOD, 700 MHz)

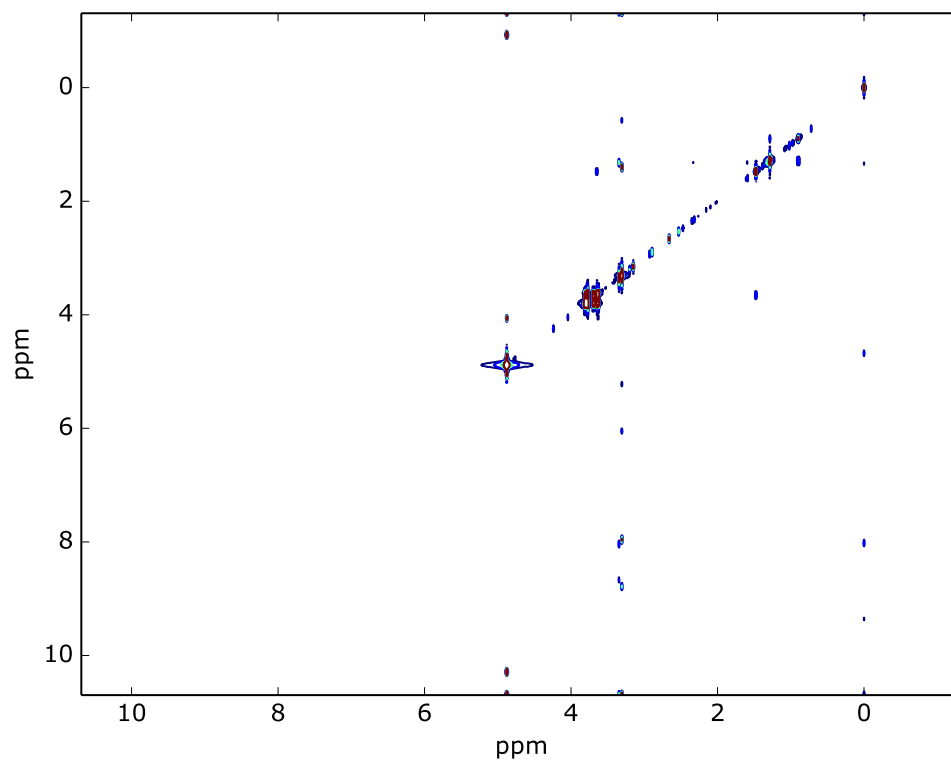
S1 - ^1H NMR spectrum (MeOD, 700 MHz)



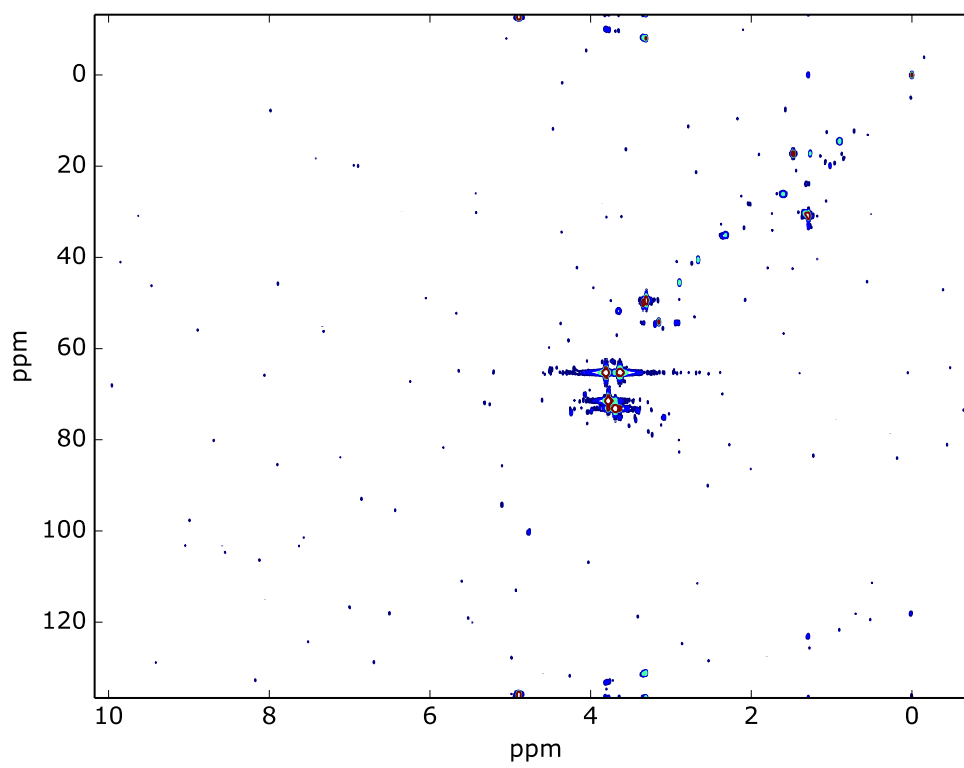
S2 - COSY spectrum (MeOD, 700 MHz)



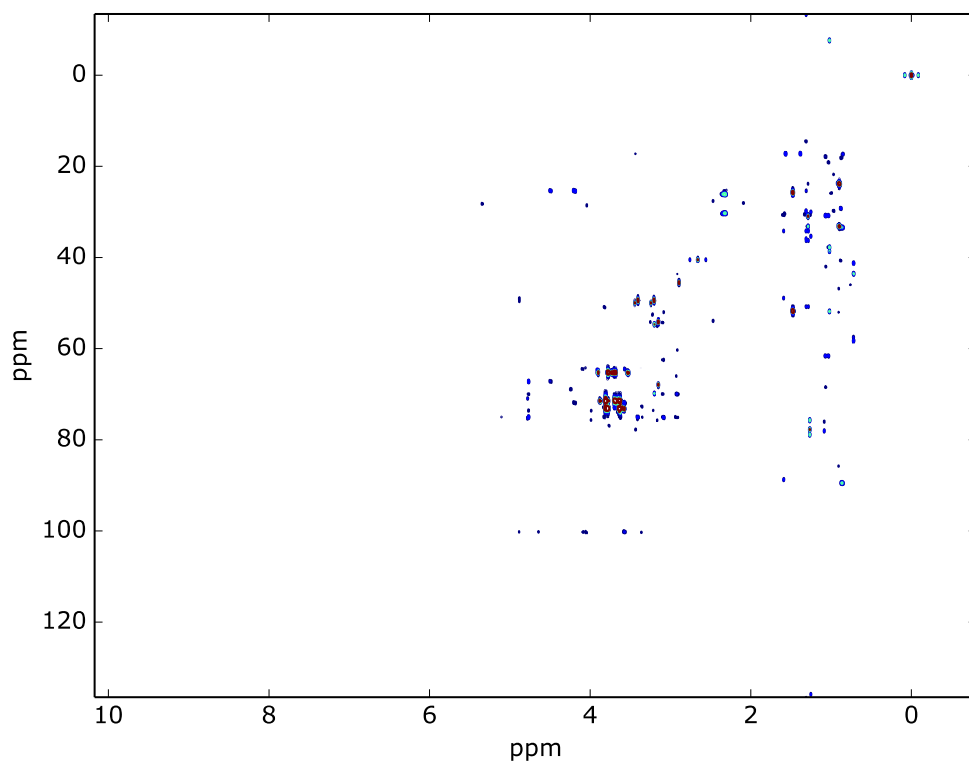
S3 - TOCSY spectrum (MeOD, 700 MHz)



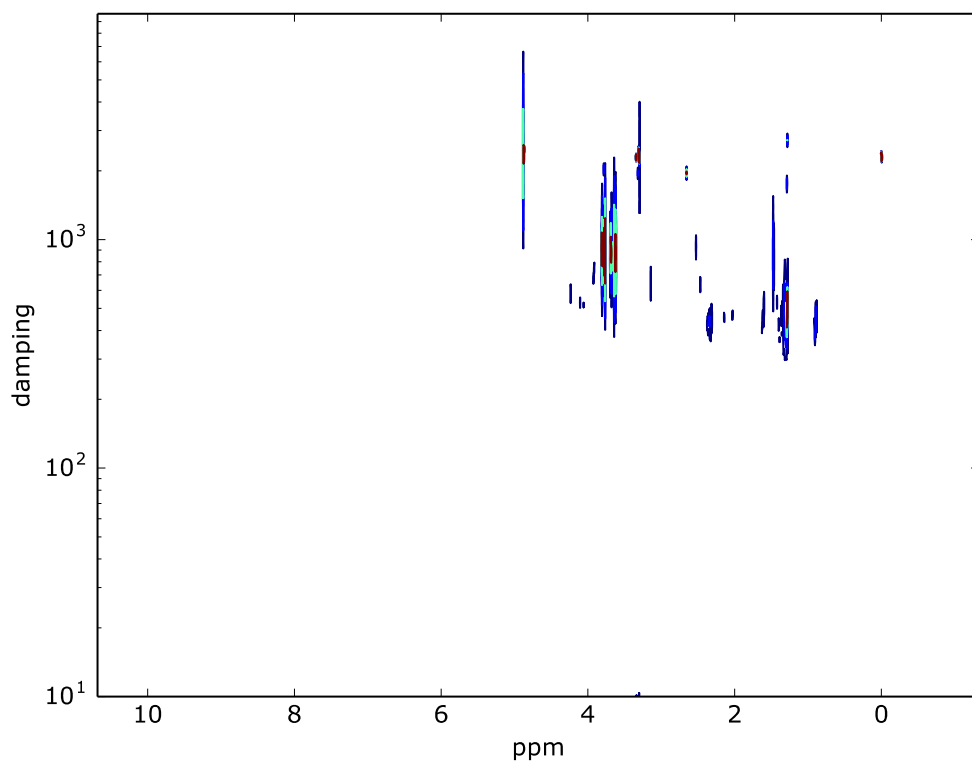
S4 - HSQC spectrum (MeOD, 700 MHz)



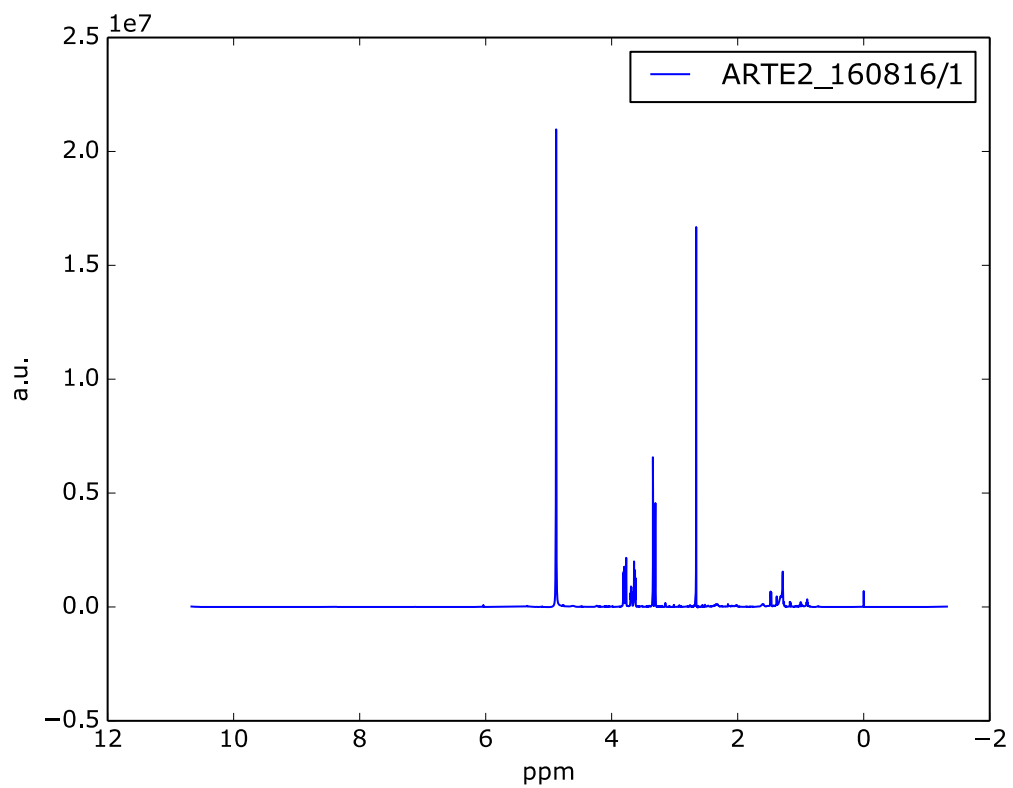
S5 - HMBC spectrum (MeOD, 700 MHz)



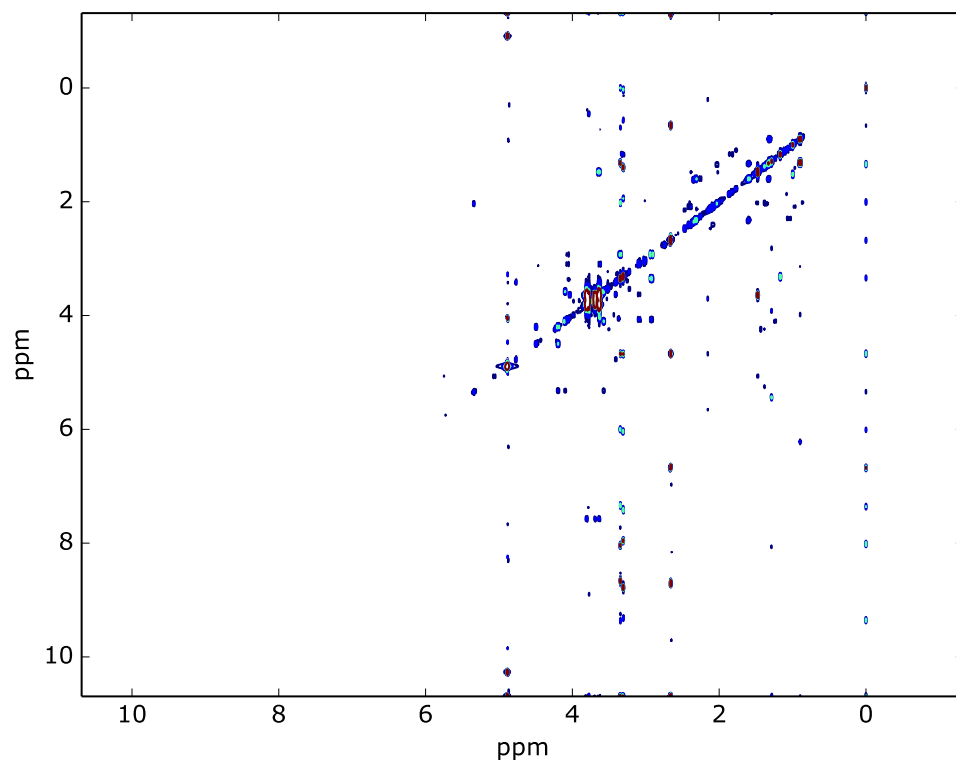
S6 - DOSY spectrum (MeOD, 700 MHz)



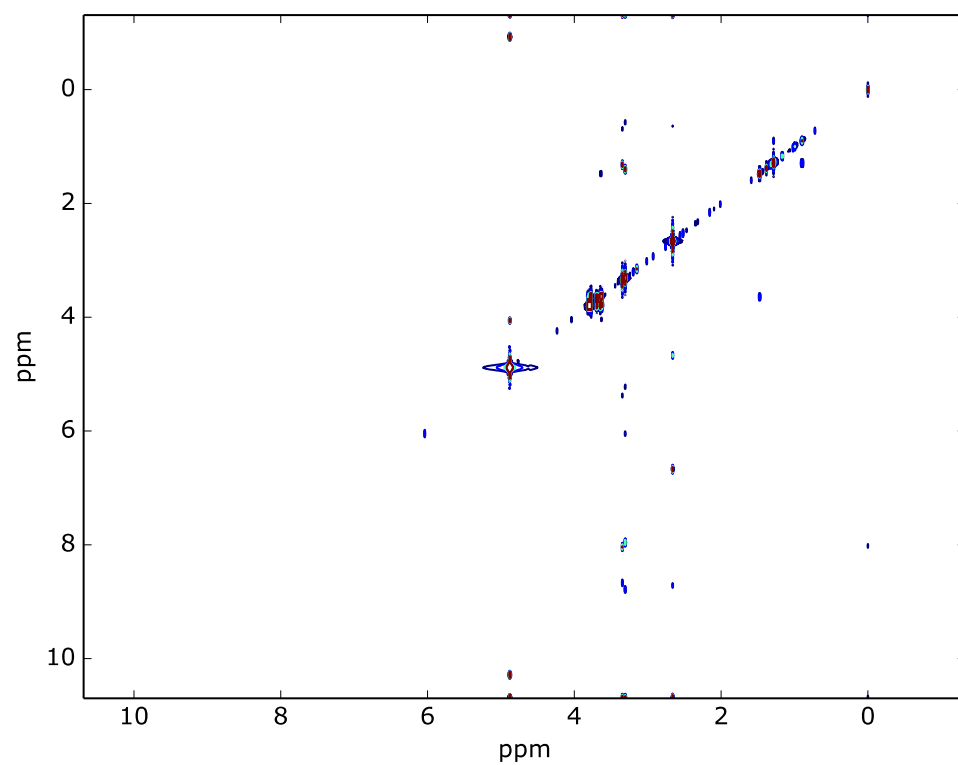
S7 - ^1H NMR spectrum (MeOD, 700 MHz)



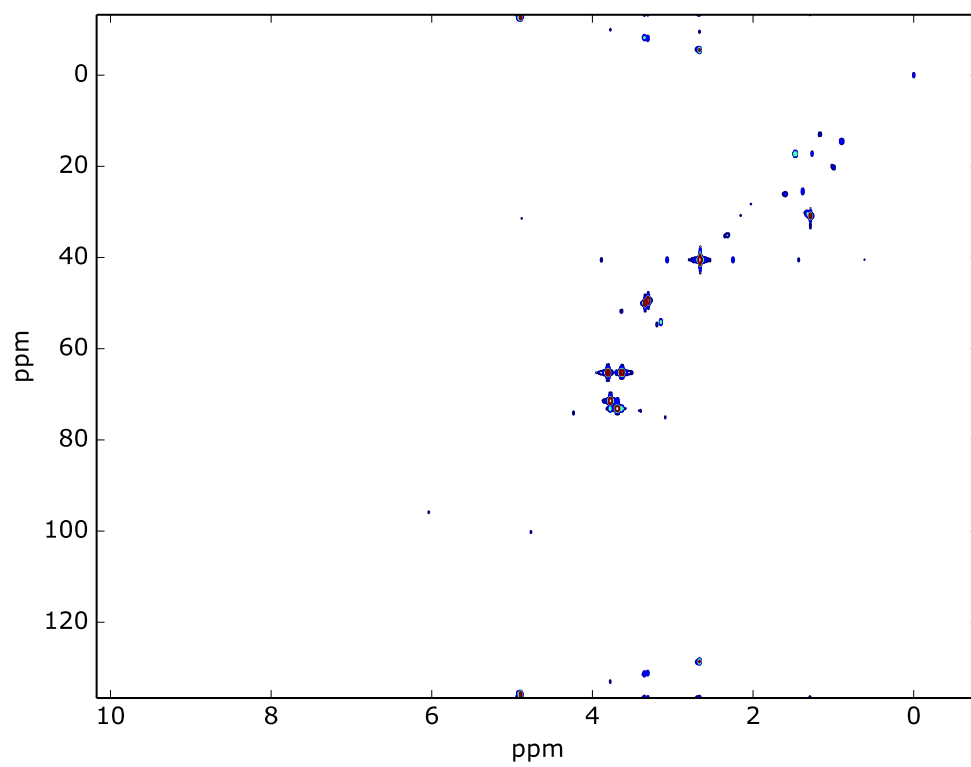
S8 - COSY spectrum (MeOD, 700 MHz)



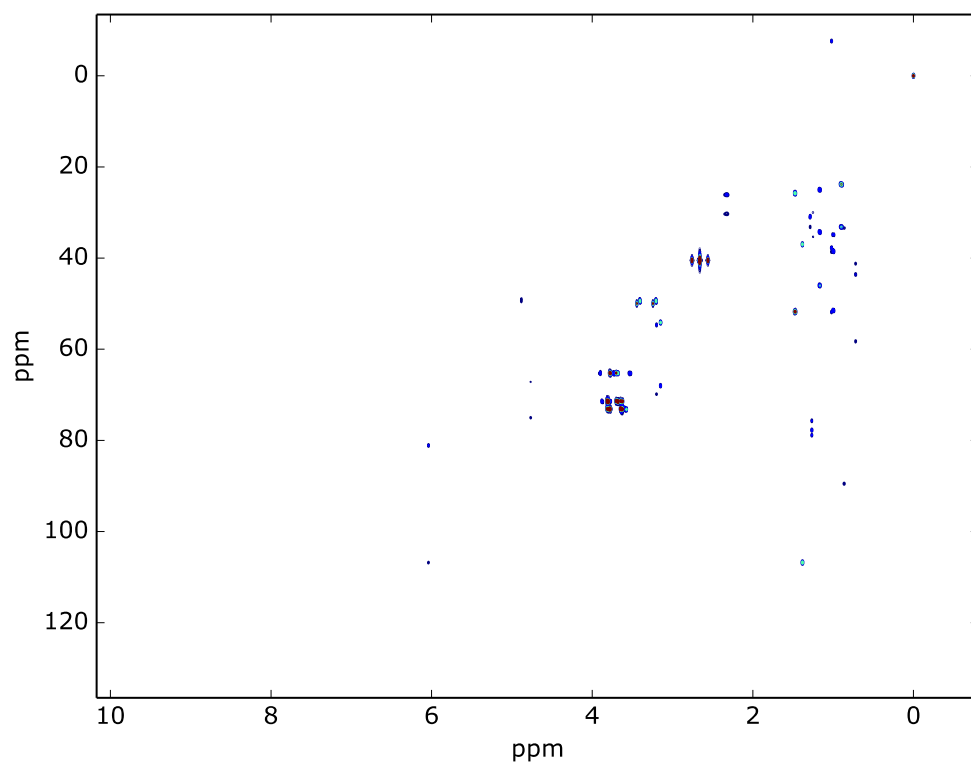
S9 - TOCSY spectrum (MeOD, 700 MHz)



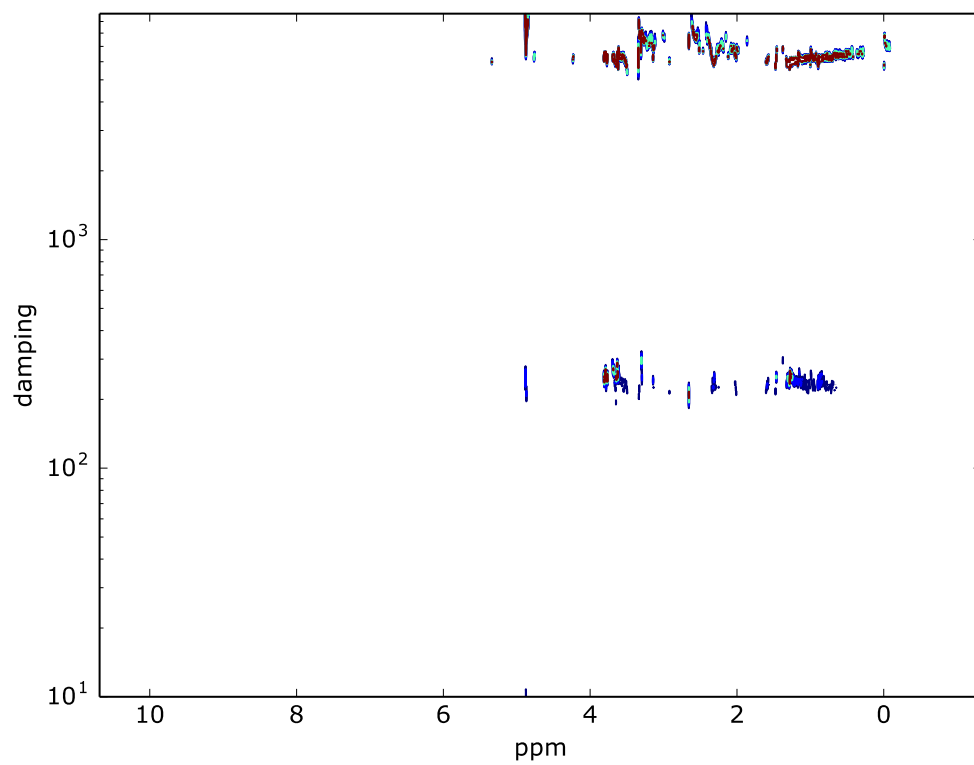
S10 - HSQC spectrum (MeOD, 700 MHz)



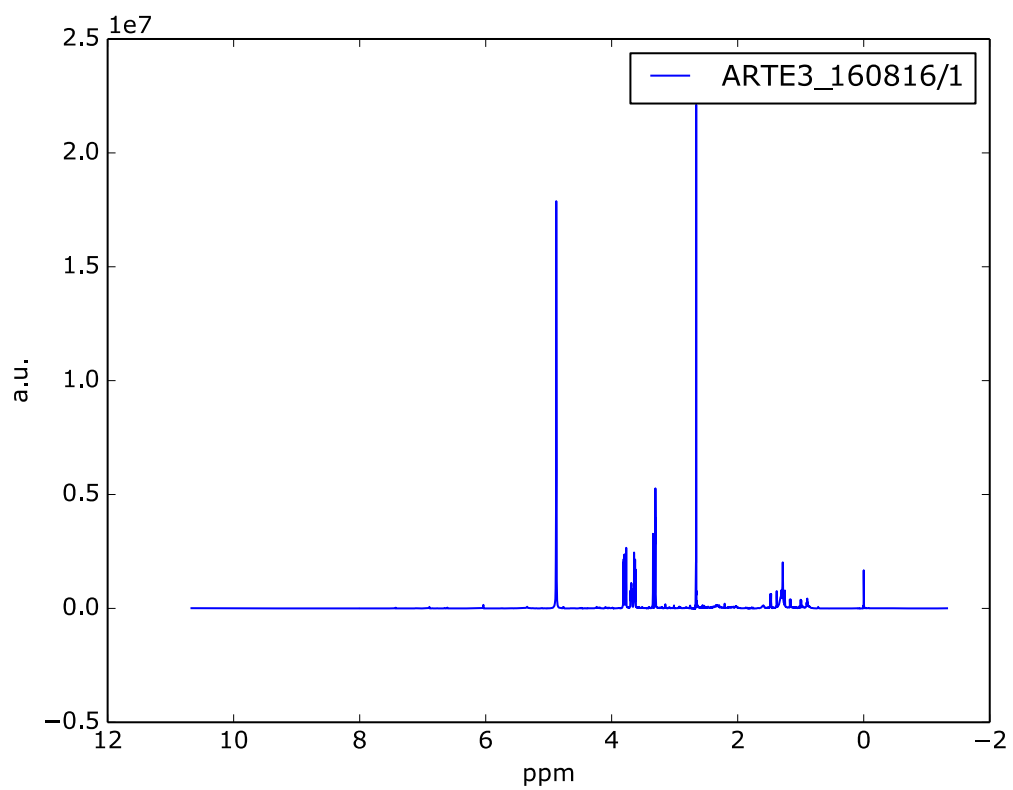
S11 - HMBC spectrum (MeOD, 700 MHz)



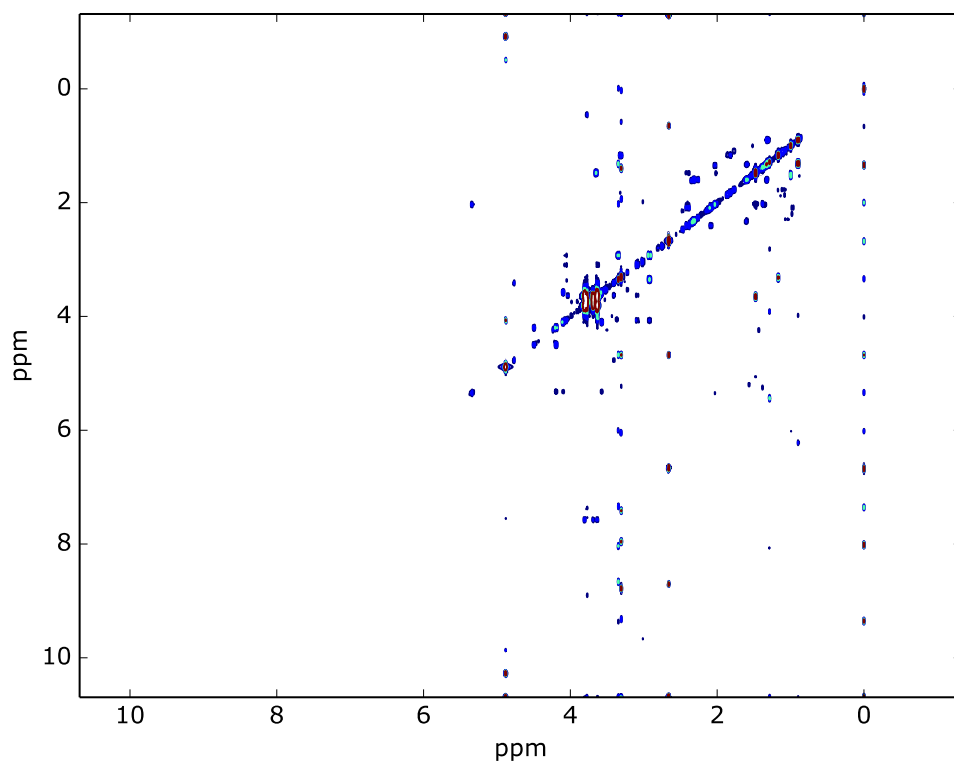
S12 - DOSY spectrum (MeOD, 700 MHz)



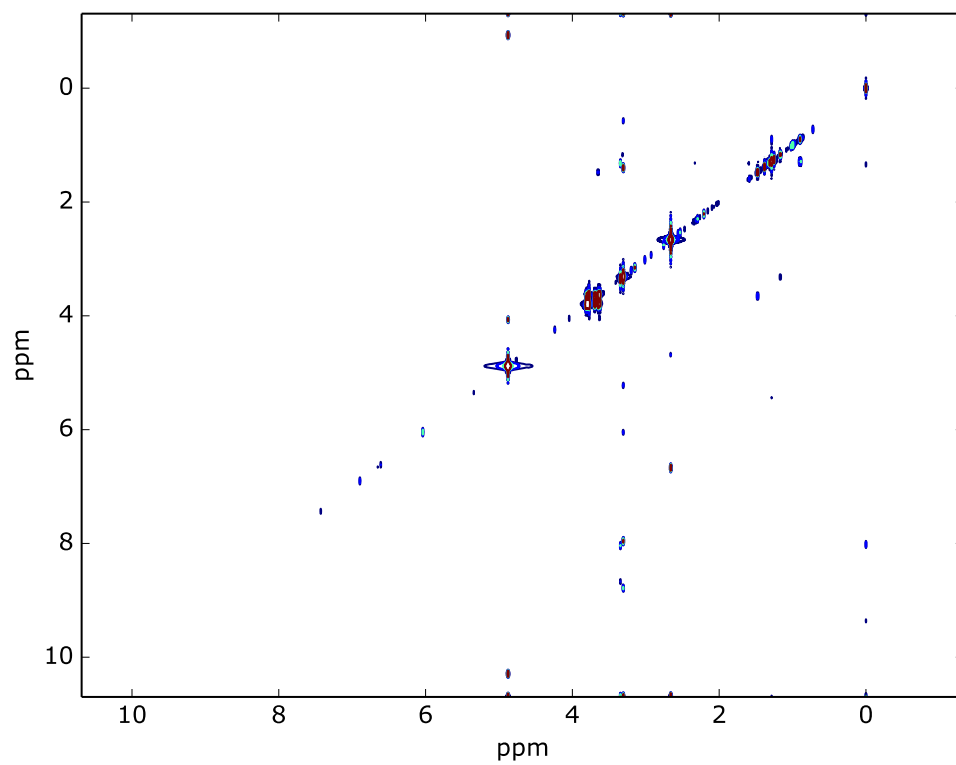
S13 - ^1H NMR spectrum (MeOD, 700 MHz)



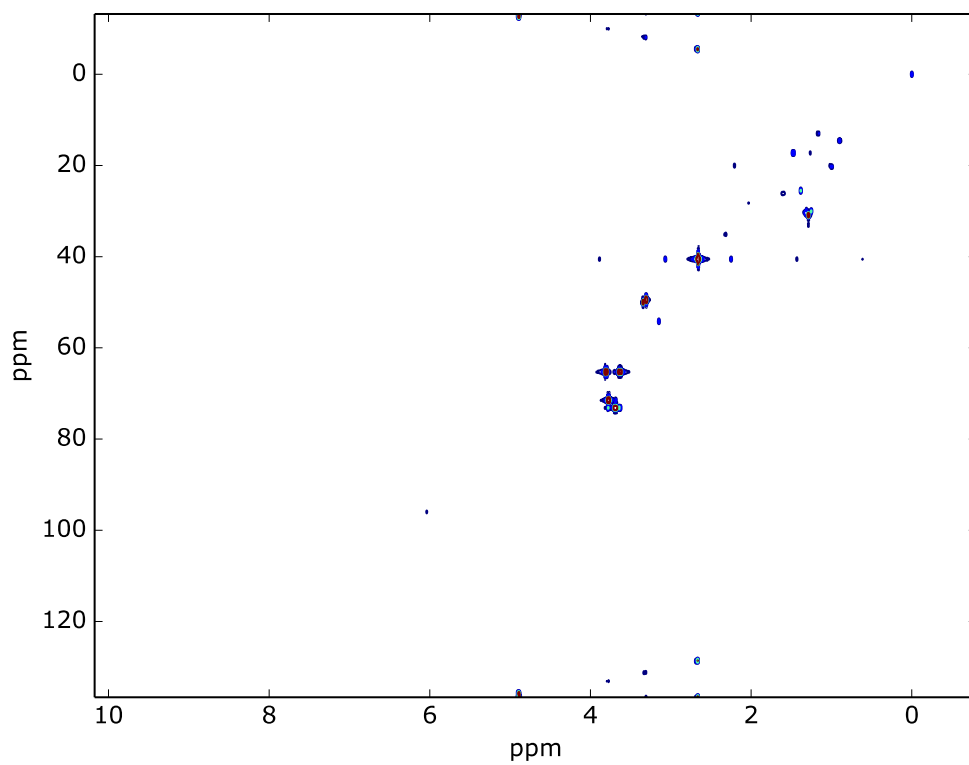
S14 - COSY spectrum (MeOD, 700 MHz)



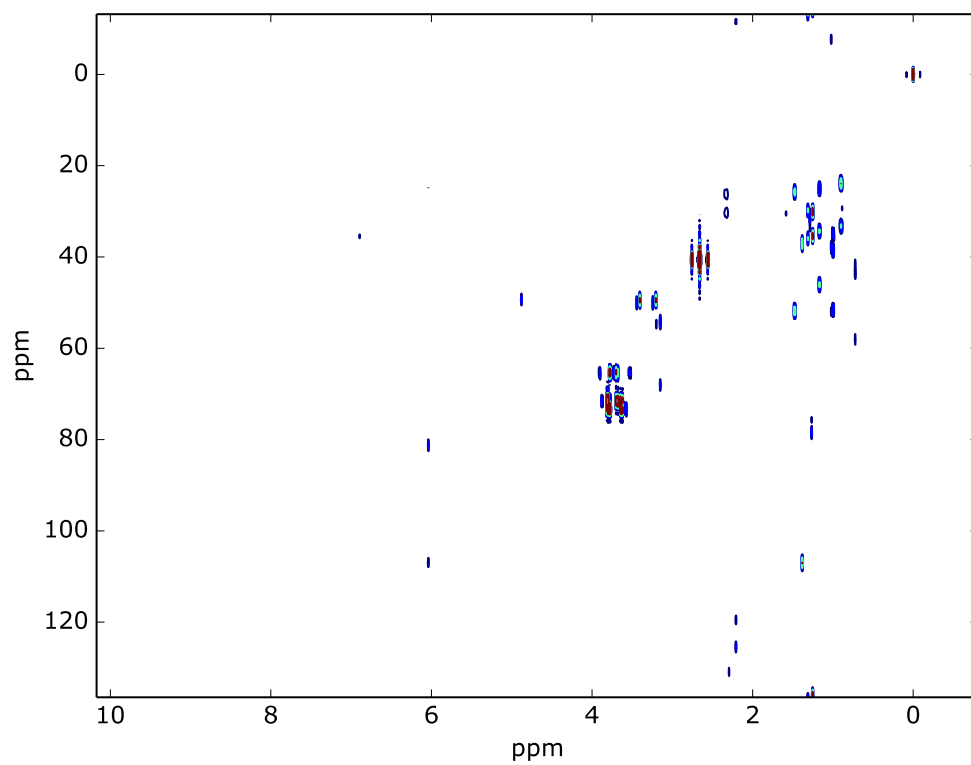
S15 - TOCSY spectrum (MeOD, 700 MHz)



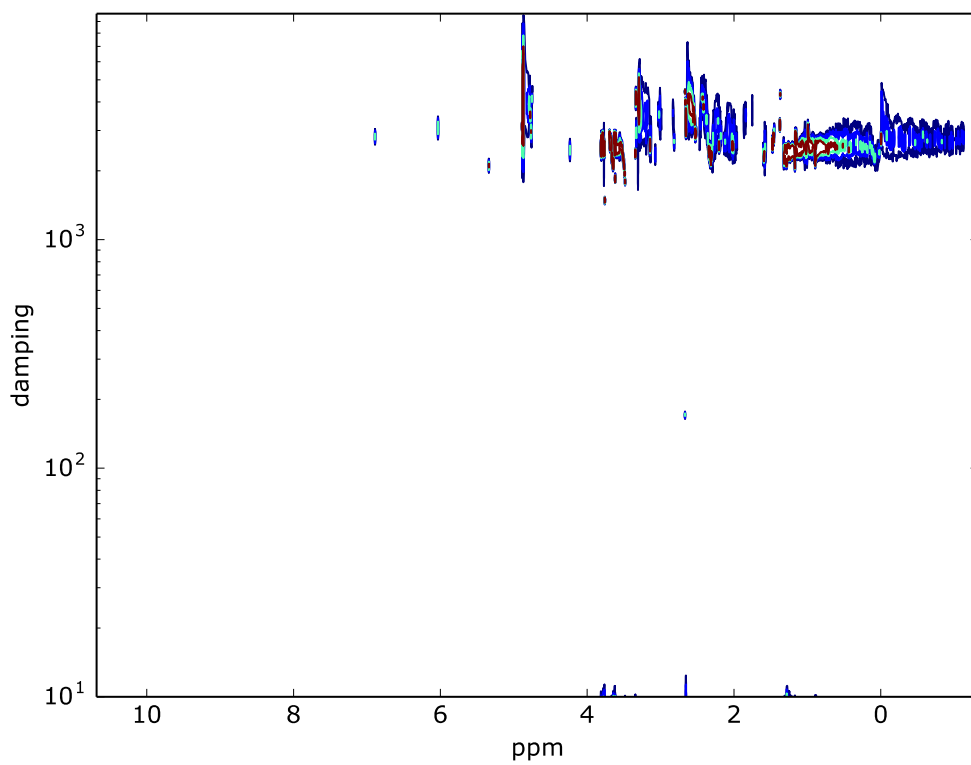
S16 - HSQC spectrum (MeOD, 700 MHz)



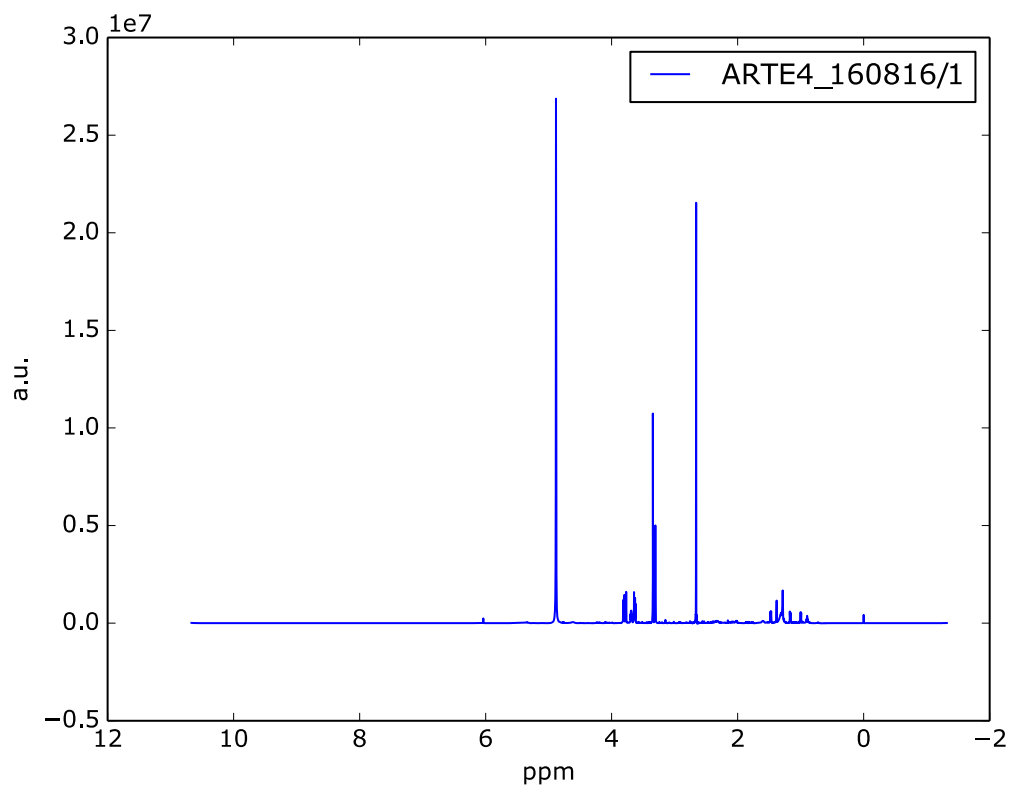
S17 - HMBC spectrum (MeOD, 700 MHz)



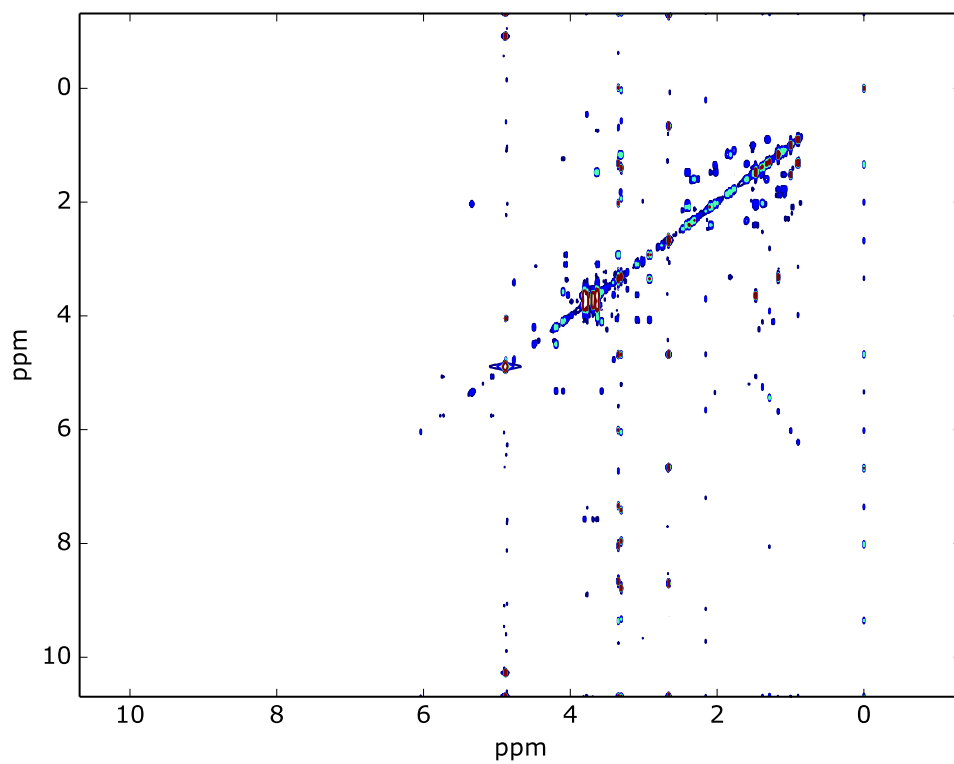
S18 - DOSY spectrum (MeOD, 700 MHz)



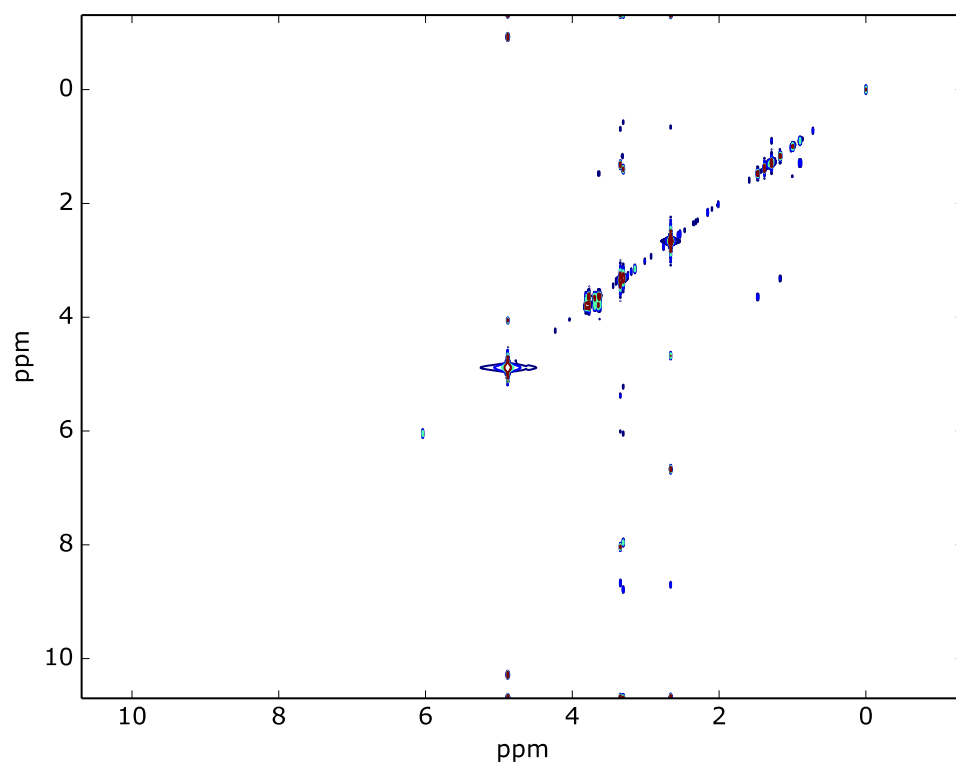
S19 - ^1H NMR spectrum (MeOD, 700 MHz)



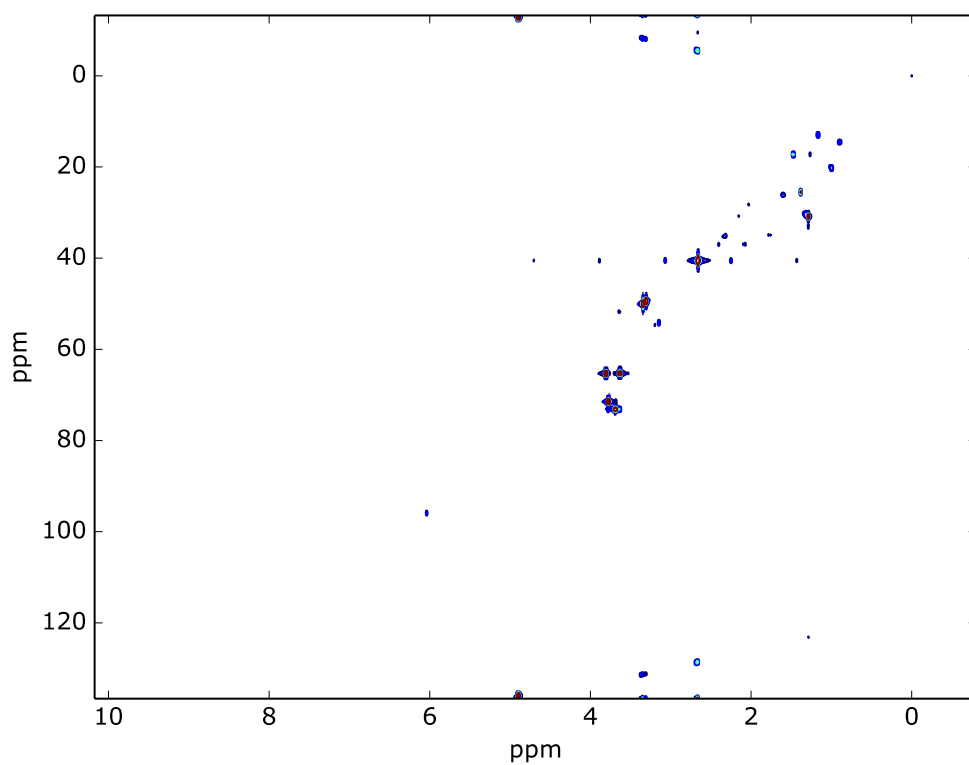
S20 - COSY spectrum (MeOD, 700 MHz)



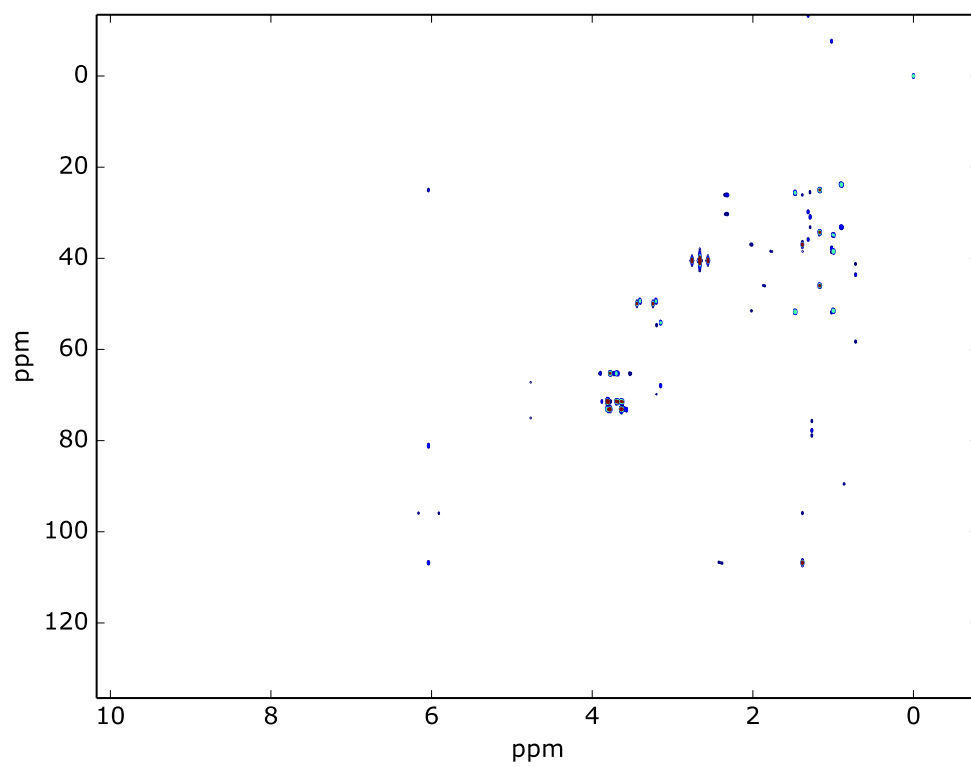
S21 - TOCSY spectrum (MeOD, 700 MHz)



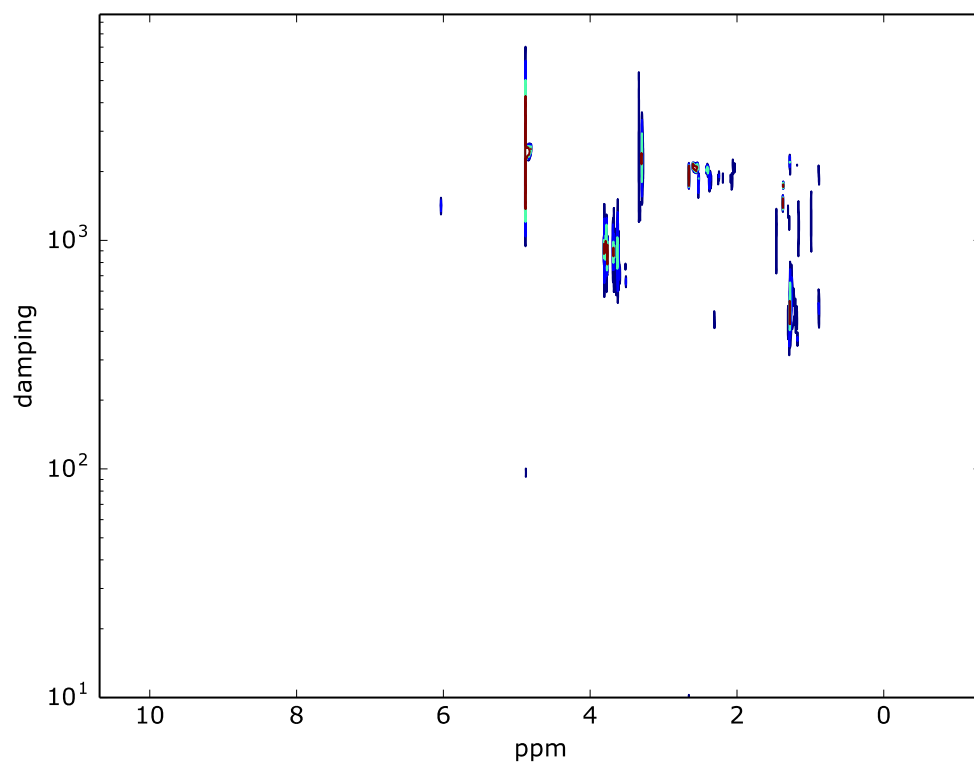
S22 - HSQC spectrum (MeOD, 700 MHz)



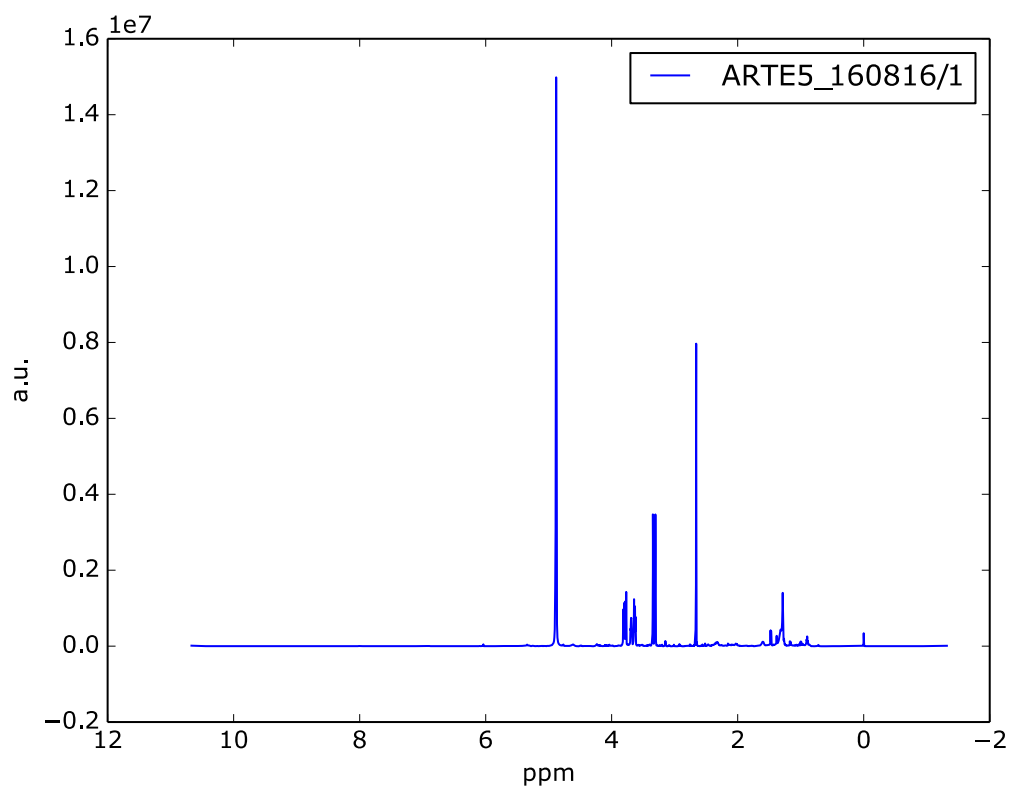
S23 - HMBC spectrum (MeOD, 700 MHz)



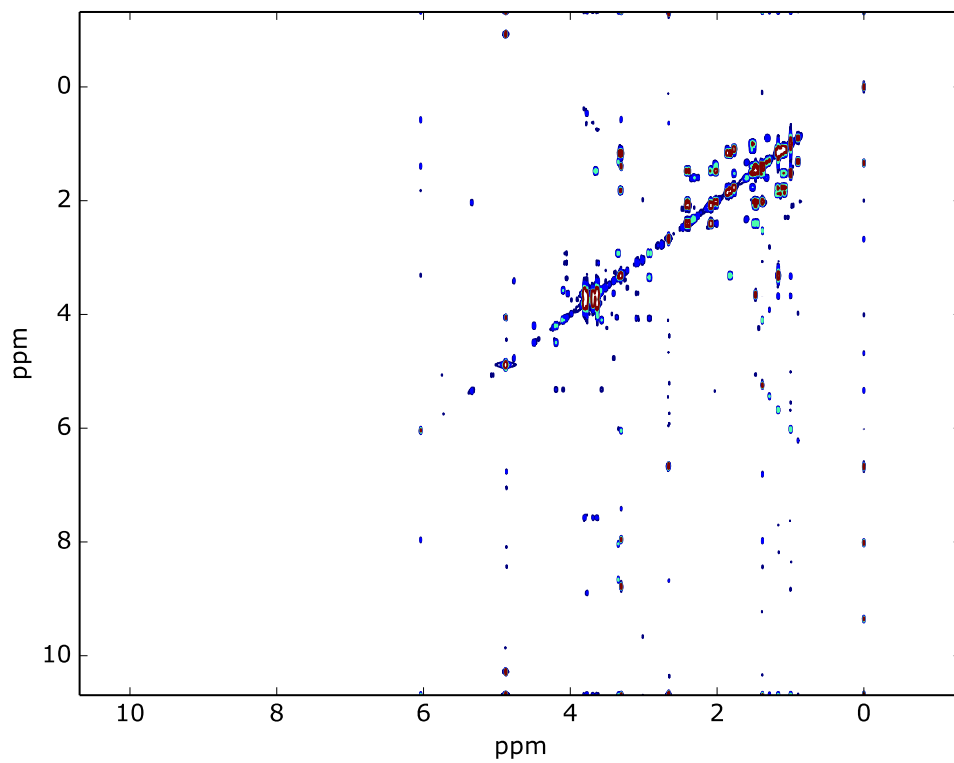
S24 - DOSY spectrum (MeOD, 700 MHz)



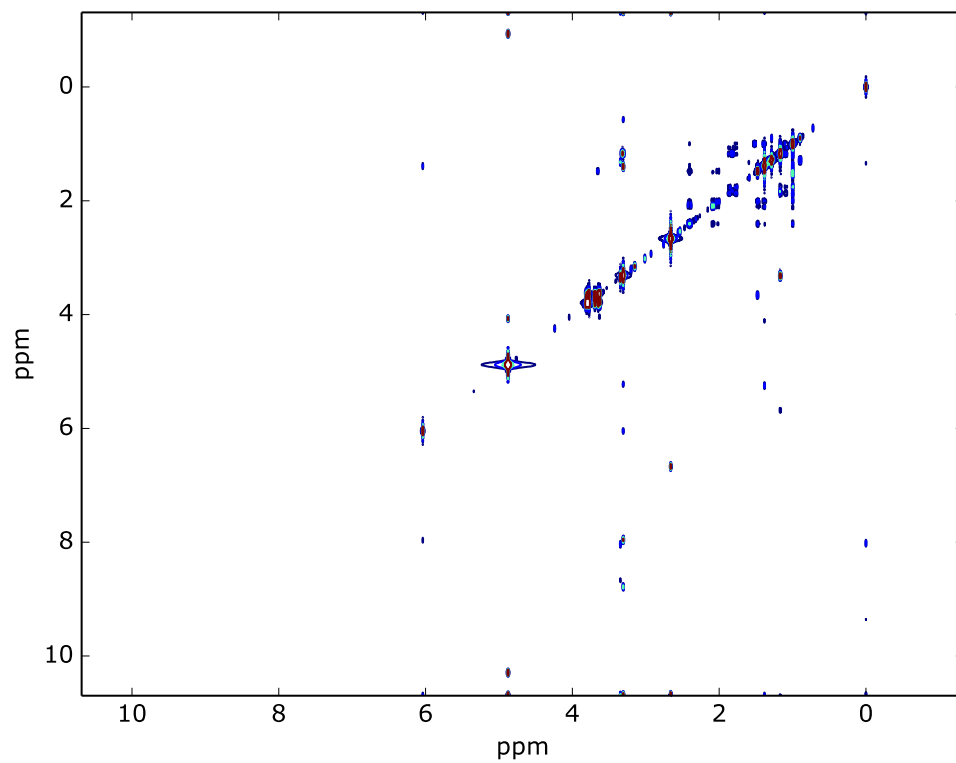
S25 - ^1H NMR spectrum (MeOD, 700 MHz)



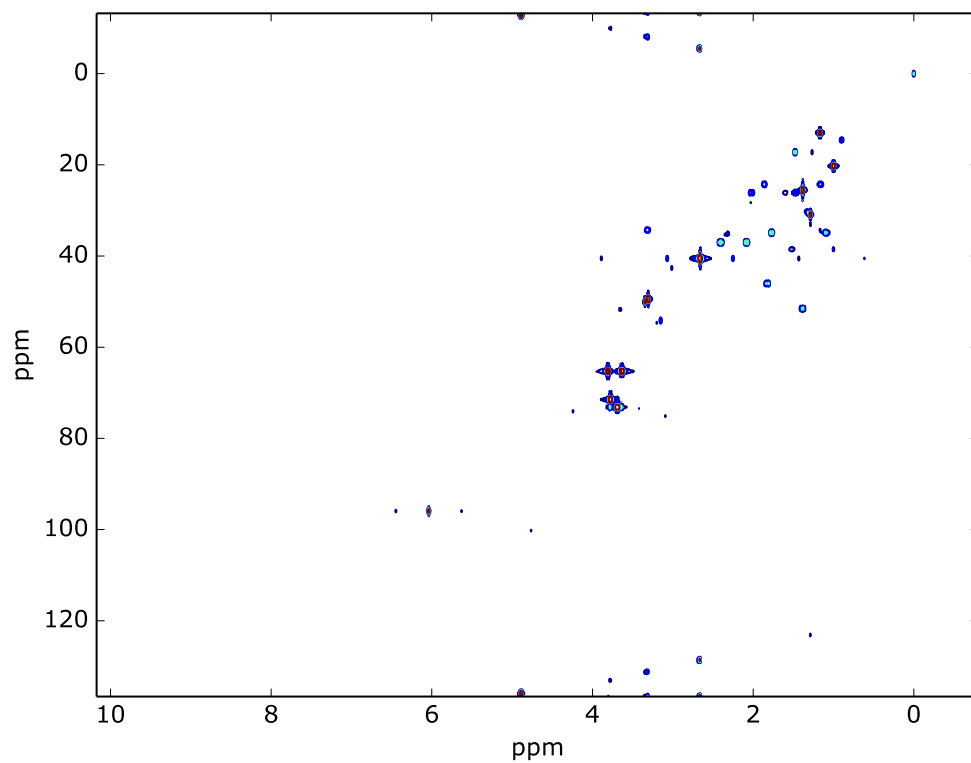
S26 - COSY spectrum (MeOD, 700 MHz)



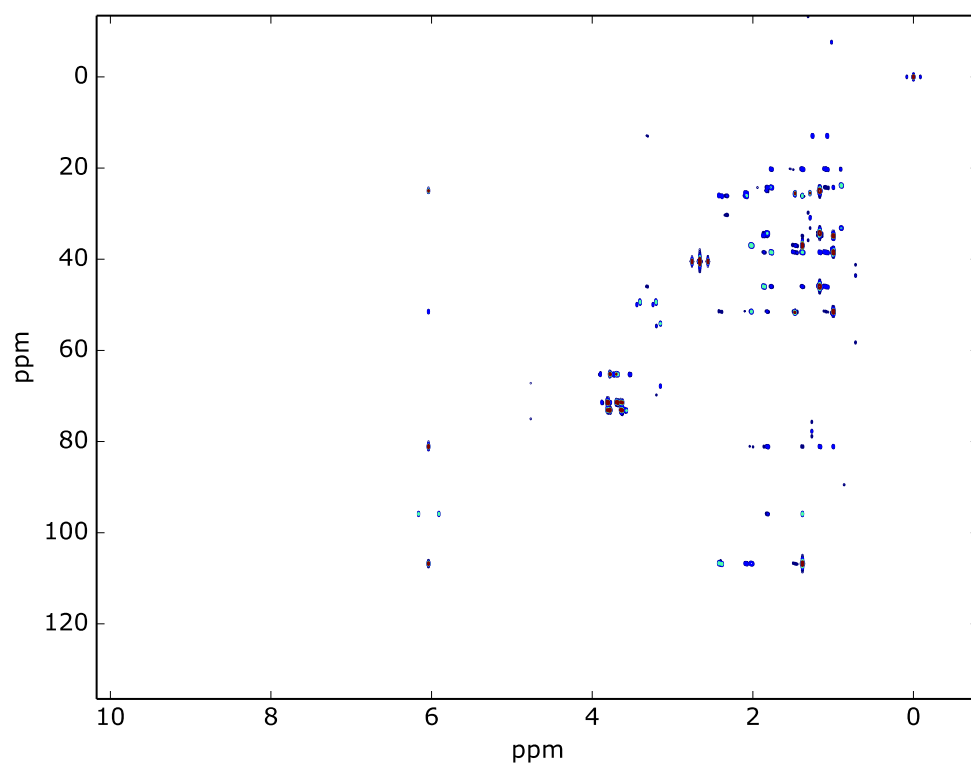
S27 - TOCSY spectrum (MeOD, 700 MHz)



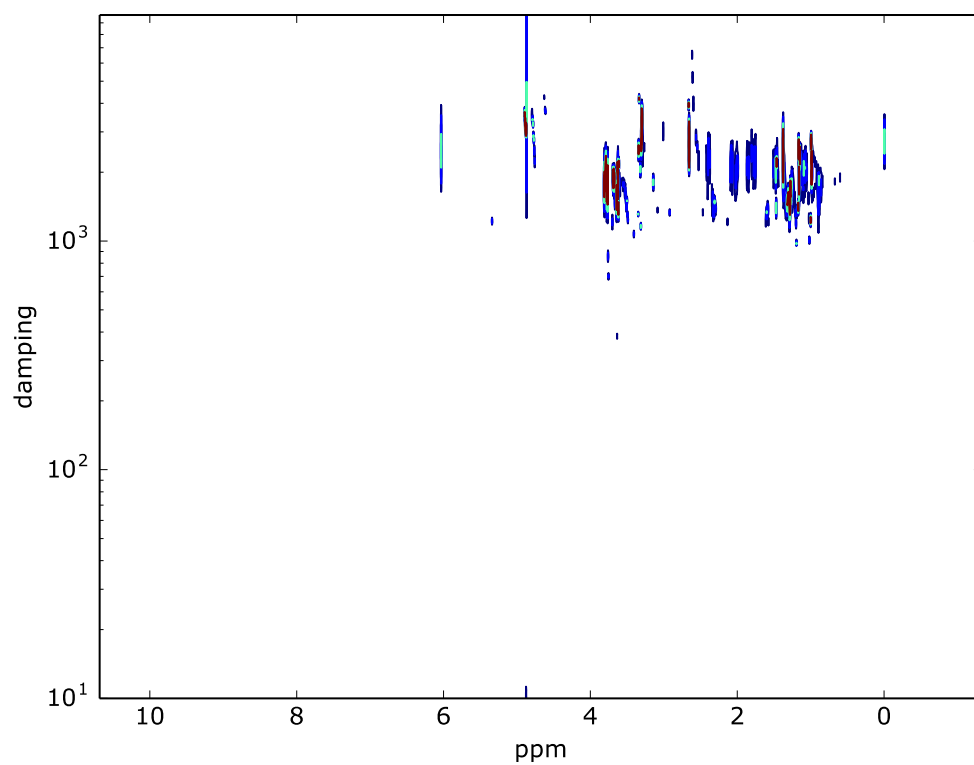
S28 - HSQC spectrum (MeOD, 700 MHz)



S29 - HMBC spectrum (MeOD, 700 MHz)



S30 - DOSY spectrum (MeOD, 700 MHz)



Supp.Info 2

Supp Info 2 can be found at <https://github.com/delsuc/plasmodesma/blob/master/Analysis.ipynb>